1999-12

Optimization procedure for electric propulsion engines

De Bellis, John J.

Monterey, California: Naval Postgraduate School

NAVAL POSTGRADUATE SCHOOL
Monterey, California

THESIS

OPTIMIZATION PROCEDURE FOR ELECTRIC PROPULSION ENGINES

by

John J. De Bellis

December 1999

Thesis Advisor: Oscar Biblarz
Co-Advisor: James Luscombe

Approved for public release; distribution is unlimited.

REPORT DOCUMENTATION PAGE

Form Approved OMB No. 0704-0188

1. AGENCY USE ONLY *(Leave blank)*	2. REPORT DATE	3. REPORT TYPE AND DATES COVERED
	December 1999	Master's Thesis

4. TITLE AND SUBTITLE
OPTIMIZATION PROCEDURE FOR ELECTRIC PROPULSION ENGINES

5. FUNDING NUMBERS

6. AUTHOR(S)
De Bellis, John J.

7. PERFORMING ORGANIZATION NAME(S) AND ADDRESS(ES)
Naval Postgraduate School
Monterey, CA 93943-5000

8. PERFORMING ORGANIZATION REPORT NUMBER

9. SPONSORING / MONITORING AGENCY NAME(S) AND ADDRESS(ES)

10. SPONSORING / MONITORING AGENCY REPORT NUMBER

11. SUPPLEMENTARY NOTES
The views expressed in this thesis are those of the author and do not reflect the official policy or position of the Department of Defense or the U.S. Government.

12a. DISTRIBUTION / AVAILABILITY STATEMENT
Approved for public release; distribution is unlimited.

12b. DISTRIBUTION CODE

13. ABSTRACT *(maximum 200 words)*

This thesis addresses the optimization of all types of space electrical propulsion thrusters. From the Langmuir-Irving payload mass fraction formulation, a "dual-optimum" solution is defined, yielding a minimum overall mass for a specified payload consistent with minimum transfer time. This solution fixes the ideal payload mass ratio (m_{pl} / m_o) at a value of 0.45, establishing the ratios of effective exhaust velocity (v / v_c) and incremental change of vehicle velocity ($\Delta u / v_c$) to characteristic velocity at 0.820 and 0.327 respectively. The characteristic velocity (v_c) includes thrust time as well as engine efficiency (η_t) and specific power (α). A range of mass ratios from 0.35 to 0.55 is used in order to allow the system designer some flexibility while remaining close to optimal. Nine examples are presented which demonstrate that mission profiles can be optimized by profile-to-thruster matching. A comprehensive list of currently available electric propulsion engines is provided. This list details important parameters such as the specific power, which "sizes" an engine in terms of power provided to the thruster at the cost of additional mass. Allowance is also made for a fuel tank mass penalty, and examples show that this can also noticeably influence the optimum design.

14. SUBJECT TERMS
Space Propulsion, Electric Propulsion, Ion Engines, Hall Thrusters, Optimum Specific Impulse, Minimum Thrusting Time

15. NUMBER OF PAGES
93

16. PRICE CODE

17. SECURITY CLASSIFICATION OF REPORT	18. SECURITY CLASSIFICATION OF THIS PAGE	19. SECURITY CLASSIFI- CATION OF ABSTRACT	20. LIMITATION OF ABSTRACT
Unclassified	Unclassified	Unclassified	UL

NSN 7540-01-280-5500

Standard Form 298 (Rev. 2-89)
Prescribed by ANSI Std. 239-18

THIS PAGE INTENTIONALLY LEFT BLANK.

Approved for public release; distribution is unlimited

OPTIMIZATION PROCEDURE FOR ELECTRIC PROPULSION ENGINES

John J. De Bellis
Lieutenant, United States Navy
B.S., United States Naval Academy, 1991

Submitted in partial fulfillment of the
requirements for the degree of

MASTER OF SCIENCE IN APPLIED PHYSICS

from the

NAVAL POSTGRADUATE SCHOOL
December 1999

Author: [redacted]
John J. De Bellis

Approved by: [redacted]
Oscar Biblarz, Thesis Advisor

[redacted]
James Luscombe, Co-Advisor

[redacted]
William Maier II, Chair
Department of Physics

THIS PAGE INTENTIONALLY LEFT BLANK.

ABSTRACT

This thesis addresses the optimization of all types of space electrical propulsion thrusters. From the Langmuir-Irving payload mass fraction formulation, a "dual-optimum" solution is defined, yielding a minimum overall mass for a specified payload consistent with minimum transfer time. This solution fixes the ideal payload mass ratio (m_{pl} / m_o) at a value of 0.45, establishing the ratios of effective exhaust velocity (v / v_c) and incremental change of vehicle velocity ($\Delta u / v_c$) to characteristic velocity at 0.820 and 0.327 respectively. The characteristic velocity (v_c) includes thrust time as well as engine efficiency (η_t) and specific power (α). A range of mass ratios from 0.35 to 0.55 is used in order to allow the system designer some flexibility while remaining close to optimal. Nine examples are presented which demonstrate that mission profiles can be optimized by profile-to-thruster matching. A comprehensive list of currently available electric propulsion engines is provided. This list details important parameters such as the specific power, which "sizes" an engine in terms of power provided to the thruster at the cost of additional mass. Allowance is also made for a fuel tank mass penalty, and examples show that this can also noticeably influence the optimum design.

THIS PAGE INTENTIONALLY LEFT BLANK.

TABLE OF CONTENTS

LIST OF FIGURES

THIS PAGE INTENTIONALLY LEFT BLANK.

LIST OF TABLES

THIS PAGE INTENTIONALLY LEFT BLANK.

LIST OF SYMBOLS AND ABBREVIATIONS

g_o	(m/s^2)	acceleration of gravity at sea level; arbitrary constant that changes units of I_s to "seconds;" $g_o = 9.81\ m/s^2$
Δu	(m/s)	incremental change of vehicle velocity
v	(m/s)	effective exhaust velocity of propellant
v_c	(m/s)	characteristic velocity; $\mathbf{v_c^2 = 2\ \alpha\ t_p\ \eta_t}$
m_o	(kg)	total initial vehicle mass; $\mathbf{m_o = m_p + m_{pl} + m_{pp}}$; $\mathbf{m_o = m_f + m_p}$
m_p	(kg)	propellant mass expelled
m_{pl}	(kg)	payload mass
m_{pp}	(kg)	power-plant mass
m_f	(kg)	final mass; $\mathbf{m_f = m_o - m_p = m_{pl} + m_{pp}}$
m_{pl}/m_o		payload fraction; $\mathbf{m_o / m_f = e^{\Delta u/v}}$
P_e	(W)	electrical power supplied to propulsion system
α	(W/kg)	specific power or "state of the art"; $\alpha = \mathbf{P_e / m_{pp}}$
I_s	(sec)	specific impulse; $\mathbf{I_s = v / g_o}$
η_t		thruster efficiency or "state of the art"
t_p	(sec, days...)	burn time
t_m	(days)	mission time – defined time for a particular Δu
T	(N)	thrust

GEO	Geosynchronous Earth Orbit – approximately 42,227 km radius
LEO	Low Earth Orbit – approximately 270 km
NSSK	North-South Stationkeeping

THIS PAGE INTENTIONALLY LEFT BLANK.

ACKNOWLEDGEMENT

I would like to express my sincere thanks and appreciation to all the professors and faculty at the Naval Postgraduate School who helped make this one of my most enjoyable tours. I would especially like to thank Professor Oscar Biblarz for his guidance and for the countless office sessions during which I came to understand the principles of electric propulsion and rocketry. Thanks, as well, to Professor Jim Luscombe for his assistance, which was invaluable in the publication of this thesis.

My most sincere thanks to the many great friends that I have met here at school. Thanks to LCDR Jon Wood for the afternoon runs, and to all my good buddies and neighbors in Pacific Grove and Carmel.

I would most especially like to give a big thank you and huge hug to my beautiful sweetie, Ms. Susana Guzmán, whose love of life and diverse interests made this thesis particularly difficult to complete.

THIS PAGE INTENTIONALLY LEFT BLANK.

I. INTRODUCTION

A. SPACE ELECTRIC PROPULSION COMES OF AGE

The application of electric propulsion for space is not a recent revolution in the field. The idea was proposed as early as the 1950's. One significant article appeared as a chapter in the text, Space Technology, entitled "Low Thrust Flight: Constant Exhaust Velocity in Field-free Space," written by D. B. Langmuir (Langmuir, 1959, pg. 9-01). Aside from the evolution of technology, little has changed in the fundamentals of electric propulsion since that time.

In the last 35 years, more than 300 electric propulsion thrusters have flown on over 100 spacecraft, and in the next decade, a significant increase in electrical propulsion employment is expected (Filliben, 1997, pg. 5). Nonetheless, electrical propulsion is only now seeing rapid and wider-scale introduction into spacecraft propulsion programs.

The first electrical propulsion engines flew in the mid-1960's. The former Soviet Union used a pulsed plasma thruster (PPT) to provide attitude control to their Zond-2/1 satellite, which launched in 1964 (Martinez-Sanchez and Pollard, 1998, pg. 692). Then, in 1965, the United States followed up their effort using a resistojet engine for orbit adjustment of the Vela/2 satellite (Martinez-Sanchez and Pollard, 1998, pg. 689).

If both of those missions proved successful, why has additional implementation of electrical propulsion for space applications been so seemingly slow, spanning almost 40 years? For this, there are both technical and doctrinal reasons.

First, engineers have only recently been able to package sufficient electrical power and power conditioning equipment onboard spacecraft in order to provide for the

demands of the electrical propulsion system. Unlike chemical propulsion, electrical requires energy accumulation and energy processing functions creating a power supply penalty at the expense of payload mass (Humble, Henry, and Larson, 1995, pg. 510). Likewise, many mission planners have been reluctant to replace proven chemical rockets with comparatively untested electrical systems. As a result, electrical systems have only gradually become accepted and only for less demanding tasks -- such as north-south station keeping (NSSK) and orbit insertion.

Nonetheless, electrical propulsion has several advantages over chemical rockets for near-zero gravity applications. Moreover, for deep-space missions, which require huge incremental changes in vehicle velocity (the factor Δu), electrical propulsion is the only realistic option. In fact, it is likely that the future of deep space exploration will depend largely upon electric propulsion systems as chemical systems will simply be unable to attain the high Δu required for these missions. Table 1 (Typical Mission Velocity Requirements) presents a summary of various mission Δu requirements.

Earth to LEO[a]	7,600 m/s
LEO to GEO[b]	4,200
LEO to Earth escape	3,200
LEO to lunar orbit (7 days)	3,900
LEO to Mars orbit (0.7 yr)	5,700
LEO to Mars orbit (40 days)	85,000
LEO to Neptune orbit (29.9 yr)	13,400
LEO to Neptune orbit (50 yr)	70,000
LEO to solar escape	8,700
LEO to 1000 AU[c] (50 yr)	142,000
LEO to Alpha-Centauri (50 yr)	30×10^6

[a] Low Earth Orbit = 270 km
[b] Geosynchronous Earth Orbit = 42,227 km radius
[c] Astronomical Units (1 AU = 149,558,000 km)

Table 1: Typical Mission Velocity Requirements. From Hill, Peterson, page 508.

Note however, that these mission velocity requirements are calculated for chemical propulsion and not electric propulsion systems. Regardless, Table 1 illustrates the typical magnitude of Δu required for various missions as the numbers do not change significantly. The values will be slightly higher for electrical systems.

On the down side, electrical propulsion systems cannot overcome high-gravity fields due to their low acceleration or low thrust. Therefore, the initial boost to attain escape velocity from Earth will need to be accomplished via chemical rockets, and it is evident that the types of missions slated for the future will be accomplished via a combination of both electrical and chemical propulsion. There are specific performance limitations to each. (Hill and Peterson, 1992, pg. 491)

Chemical rockets can be described as "energy limited" in that the fundamental chemical behavior of the propellant defines the quantity of energy (per unit mass of propellant) that can be released during combustion. High propellant energy for spacecraft is possible if a separate energy source is utilized -- such as nuclear or solar energy. In that manner, the rate of conversion of nuclear or solar energy to electrical and then to propellant kinetic energy is limited by the mass of conversion equipment required. That mass can be a comparatively large portion of the total vehicle mass. As a result, the electrical rocket is generally said to be "power limited." (Hill and Peterson, 1992, pg. 491)

B. PHYSICS BEHIND ELECTRIC PROPULSION

Space electrical propulsion systems consist of three basic subsystems. Those subsystems include the power processing unit, propellant management assembly, and the thruster assembly consisting of one or more thrusters.

The power processing unit (PPU) contains electrical interfaces that link the spacecraft power source and the propulsion system. The PPU sends power and command signals to the thruster(s) and propellant flow control signals to the propellant subsystem. Additionally, the PPU is responsible for converting various power sources (solar, batteries, fuel cells, nuclear, etc.) to the proper voltage, frequency, pulse rate, and current suitable for the system components.

The propellant management assembly (PMA) provides the means of storing, metering and delivering the propellant. The thrusters convert electrical energy to kinetic energy of a propellant in the form of exhaust or thrust.

Regardless of type, the common feature of electric propulsion systems is the addition of energy to a working fluid from an electrical source. Operating in a steady or pulsed mode, the exhaust is accelerated via one or more of the three fundamental types of thrusters. Those types of thrusters are (1) electrothermal, (2) electrostatic, and (3) electromagnetic. (Martinez-Sanchez and Pollard, 1998, pg. 688)

In reading the following sections, reference Figure 1, "Operating Principles of Various Electrical Propulsion Thrusters," found at the end of this chapter on page 14. The figure will prove exceptionally useful in understanding the operation of several of the following thrusters as they are discussed.

1. Electrothermal Thrusters

In the electrothermal thruster, the propellant is electrically heated and thermodynamically expanded. The heated gas then achieves supersonic velocity as it passes through a nozzle. Overall, these thrusters have one major drawback in that, as a class, they produce limited high exhaust velocities. Additionally, their material

characteristics limit their performance to values that are generally in line with those exhibited by chemical rockets. At present, there are two basic types of electrothermal thrusters -- resistojets and arcjets.

The resistojet is the more elementary of the two in its class. In essence, it operates by using an electric current to directly heat metal components (coiled wire, tubing, or fins) which then transfer heat to the gaseous propellant through radiation and/or convection. As a result, the resistojet's performance is limited by the capacity of its structural components to withstand high temperatures, and resistojets achieve only a modest specific impulse of 300-310 seconds. This is due to the relatively high molecular mass of the propellant gas in addition to material limitations of the heating wall, which can sustain temperatures up to approximately 2000 K. (Martinez-Sanchez and Pollard, 1998, pg. 689)

Even with its comparatively lower value of specific impulse, the resistojet's superior efficiency contributes to far higher values of thrust/power than other varieties of electrical propulsion. Additionally, these engines possess the lowest overall system "dry mass" since they do not require a power processor and their plumes are uncharged. (Sackheim and Byers, 1998, pg. 672)

Resistojets have seen successful employment on such craft as Intelsat V, Satcom 1-R, GOMS, Meteor 3-1, Gstar-3, and Iridium S/C in addition to older satellites and test flights (Martinez-Sanchez and Pollard, 1998, pg. 689). They are most attractive to the mission planner for low-to-modest energy applications. In particular, they are most suitable where power limits, thrusting times, and plume impacts are mission drivers. (Sackheim and Byers, 1998, pg. 672)

The other form of the electrothermal thruster, the arcjet, manages to overcome the thermal problems encountered by the resistojet, and it enables a significant increase (approximately double) in specific impulse over the resistojet. The arcjet accomplishes this by forming an attached arc within the nozzle that directly heats the propellant stream to temperatures much greater than those encountered at the thruster body. Essentially, the power is deposited internally in the form of the electric arc, which typically operates between a concentric upstream rod cathode and a downstream anode that serves as a supersonic nozzle. (Martinez-Sanchez and Pollard, 1998, pg. 689)

The arc core reaches temperatures of 10-20,000 K while the buffer layer near the wall is maintained at less than 2000 K. As a consequence of the temperature gradient, there is practically no propellant flow through the arc core. This results in high specific impulse at the cost of reduced propulsive efficiency. In addition, the flow structure at the throat is extremely non-uniform, and the thruster is primarily limited by arc instabilities and erosion of the nozzle. (Martinez-Sanchez and Pollard, 1998, pg. 689) Generally, arcjets exhibit significant decreases (approximately six times) in thrust/power relative to the resistojet. This is due to an increased specific impulse coupled with relatively low values of efficiency ranging from 0.3 to 0.4. (Sackheim and Byers, 1998, pg. 672)

One significant disadvantage to the arcjet is that the required PPU is substantially more complex than that encountered in the resistojet as the complex plasma arc must be controlled. In fact, the PPU may be several times heavier than the thruster itself. Still, however, the arcjets exhibit relatively low dry masses when compared with some of the other electrical propulsion systems in use or development. (Martinez-Sanchez and Pollard, 1998, pg. 689)

With its intermediate specific impulse of 600 - 650 seconds, the arcjet is a very viable option for short burn duration missions. The lower specific impulse implies higher thrust for a given power, and arcjets have been used for geostationary applications, including the Telstar 4 and GE-1 satellites. (Martinez-Sanchez and Pollard, 1998, pg. 689) The engines are relatively simple to integrate, and they are the least costly and complex of any plasma propulsion device (Sackheim and Byers, 1998, pg. 672).

2. Electrostatic Thrusters

Electrostatic thrusters rely on electrostatic fields in order to exert forces on the propellant which is throttled into the field in the form of charged particles. Such thrusters can only operate in a vacuum, and all the created particles must be of the same sign -- i.e. all positive or all negative. Likewise, those particles must be neutralized after passing through the engine. Otherwise, the thruster would eventually render itself ineffective as a net charge would build up on the spacecraft setting up the return of oppositely charged ions to the craft. As a result, any thrust would be cancelled. In addition, sensitive system components could be damaged by the returning ions. (Humble, Henry, and Larson, 1995, pg. 532)

Naturally, electrons would seem to be the most likely candidate particles for these engines. They are easy to produce and to accelerate; however, their small mass renders them impractical. They are, in fact, so extremely light that the momentum imparted to them is negligible even with their high velocity.

Consequently, electrostatic thrusters operate using heavy atoms charged as positive ions or as colloids (liquid droplets). Neutralization of the positive ions is easily accomplished with electrons, and the ions can be 240,000 times as heavy as the electron.

The charged colloids are generally at least 10,000 times as massive as the ions. Thus, substantial momentum can be generated.

The implementation of heavy atoms has other advantages. The thrust per unit area increases as the square of the particle mass to the charge ratio in addition to the highly desirable characteristic of high voltage and low current as opposed to low voltage and high current (Sutton, 1992, pg. 580).

Electrostatic thrusters are categorized by the source of charged particles, and all three types exhibit the same three basic stages: ion production, acceleration, and neutralization. The five types of thrusters that have been studied are as follows:

1. Electron Bombardment Ion Thruster. Positive ions are produced via the bombardment of vaporized or gaseous propellant (such as xenon or mercury) with electrons emitted from a heated cathode.
2. Ion Contact Thruster. Positive ions are created by passing a propellant vapor (cesium) through a hot contact ionizer (usually tungsten). Although it was intensely investigated 15 to 30 years ago, the ion contact thruster was abandoned as impractical.
3. Field Emission (Colloid) Thruster. This engine generates positive or negative particles by passing tiny liquid droplets of propellant through an intense electric field (corona discharge). (Sutton, 1992, pg. 580)
4. Radio Frequency Ion Thruster. This thruster produces a high specific impulse at the price of complexity and mass. Essentially, it consists of a discharge chamber that is surrounded by an inductive coil connected to a radio frequency generator. Neutral propellant atoms are ionized by the

bombardment of electrons which are accelerated by the induced high-frequency eddy fields in the discharge chamber.

5. Electron Cyclotron Resonance / Microwave Discharge Ion Thrusters. Here a circularly polarized microwave beam is projected from a conventional waveguide via a suitable dielectric window in order to ionize the propellant in the discharge chamber. (Filliben, 1997, pg. 5)

At the present time, ion engines are the "thruster of choice" for deep missions such as interplanetary transfers. These missions require a high Δu and must tolerate long thrusting times. (Martinez-Sanchez and Pollard, 1998, pg. 692) A typical xenon ion thruster can generate an average mission specific impulse of 2,800 - 3,500 seconds with a lifetime of greater than 8000 hours (333 days).

3. Electromagnetic Thrusters

There are several variations to the electromagnetic type of thruster. All make use of a propellant gas that is heated to a plasma state. That plasma is then part of a current-carrying electric circuit which interacts with combined electric and magnetic fields thereby generating thrust.

The four types of electromagnetic thrusters which we will discuss include the Hall-effect thruster, stationary plasma thruster (SPT), the magnetoplasmadynamic (MPD) thruster, and the pulsed plasma thruster (PPT).

The Hall-effect thruster is named for its closed circular electron drift that is exhibited between the cathode and anode of the thruster. This effect is analogous to the Hall Effect. The SPT operates on similar principles.

In the Hall-effect thruster, an axial electric field and radial magnetic field are established in the discharge chamber. Meanwhile, neutral propellant atoms are fed into the discharge chamber and ionized by the bombardment of electrons. The perpendicular electric and magnetic fields then force the electrons, emitted from an external hollow cathode, to become trapped in azimuthal drift motion. At the same time, the radial magnetic field is not sufficiently strong to affect the propellant ion trajectory, and they are consequently accelerated axially by the electric field, producing thrust. (Filliben, 1997, pg. 5)

The first use of a Hall thruster electric propulsion system in space took place in October of 1998. The U. S. Navy's Hall thruster, installed on an experimental spacecraft owned by the National Reconnaissance Office, began operating as part of the electric propulsion demonstration module (EPDM). The engine provides for orbit raising and long-term station keeping. (Space Tracks, 1999, pg. 13)

The particular engine onboard the EPDM is a TAL (thruster with anode layer) type Hall thruster, using xenon gas. It is a gridless device producing greater than twice the thrust of an ion engine of the same operating power. (Space Tracks, 1999, pg. 13)

Although still in development, the magnetoplasmadynamic thruster (MPD) is generally regarded as the leading potential candidate for future deep space missions such as a heavy-lift Mars transfer, utilizing a nuclear powerplant. (Martinez-Sanchez and Pollard, 1998, pg. 693)

The engine operates by generating a current along a conducting bar. The current consequently yields a self-induced azimuthal magnetic field that interacts with the current of an arc that travels from the point of the bar to a conducting wall. The resulting force

has two components. One component is a radially inward force that constricts the flow, and the other force acts along the axis, producing directed thrust. As expected, one of the great problems with this thruster is the substantial erosion that occurs at the point of contact between the arc current and electrodes. (Santarius, 1997) Additionally, the MPD thruster is more difficult to optimize due to the fact that several physical effects are involved in its operation.

The Pulsed Plasma Thruster (PPT) is "different from all other concepts" in two fundamental ways. This device operates in short pulses of approximately 10 microseconds duration, and in its most developed form uses a portion of solid propellant feedstock (typically Teflon®). As a result, no propellant tanks (referred to as "tankage") are required in this device. (Martinez-Sanchez and Pollard, 1998, pg. 692)

In the PPT, a portion of the feedstock is ablated and ionized by an electrical arc discharge sheet initiated between two electrodes by a discharging capacitor. The resulting propellant plasma is accelerated by the interaction of the arc and the self-induced magnetic field of the current loop. (Filliben, 1997, pg. 5)

The PPT design is comparatively simple and reliable. However, one of the inherent problems with this thruster is that the force falls off as the current loops get large. In addition, PPT's generally suffer from low efficiencies on the order of 8 to 13 percent. (Santarius, 1997)

PPT's offer two additional distinct advantages in that they integrate a non-toxic propellant feed system with a thruster in a single compact unit as well as offering a variable pulse repetition rate. As a result, they possess a flexibility of operation over a wide range of mean power or thrust, and therefore, they have found employment for

precision orbital or attitude-control tasks since the late 1960's with the LES-6 satellite and the U. S. Navy's NOVA constellation. (Martinez-Sanchez and Pollard, 1998, pg. 692)

The *optimal* implementation of these three fundamental types of electric propulsion engines (electrothermal, electrostatic, and electromagnetic) will be the focus of our analysis. As illustrated in this chapter, there are several variants of each of the engines. Some of those engines are currently in use or in various stages of development. Please reference Table 2 on page 13 for a summary of typical electrical propulsion performance parameters.

Type	Thrust (mN) / Duration	I_s (sec)	Efficiency[a]	Specific Power (W/mN)	Typical Propellants
Electrothermal:					
Resistojet	200 - 300 / months	200 - 350	0.65 - 0.9	0.5 - 6	NH_3, N_2H_4, H_2
Arcjet	200 - 1000 / months	400 - 1000	0.3 - 0.5	2 - 3	H_2, N_2, N_2H_4, NH_3
Electrostatic:					
Ion Engine	0.01 - 200 / months	1500 - 4000	0.6 - 0.8	10 - 70	Xe, Ar, Kr
Electromagnetic:					
Solid Pulsed Plasma	0.05 - 10 / years	1000 - 2000	0.2 - 0.3	10 - 50	Teflon
MPD Arcjet	0.001 - 2000 / weeks	1000 - 8000	0.1	100	Ar, Xe, H_2
Hall Effect	0.01 - 2000 / months	2000 - 5000	0.3 - 0.5	100	Xe
Monopropellant rocket[b]:					
	30 - 100,000 / hrs., mins.	200 - 230	0.87 - 0.97	N/A	N_2H_4

[a] Efficiency = thrust-power output / electrical-power input
[b] Listed for comparison only.

Table 2: Typical Performance Parameters of Various Types of Electrical Propulsion Systems. Adapted from Sutton, page 567.

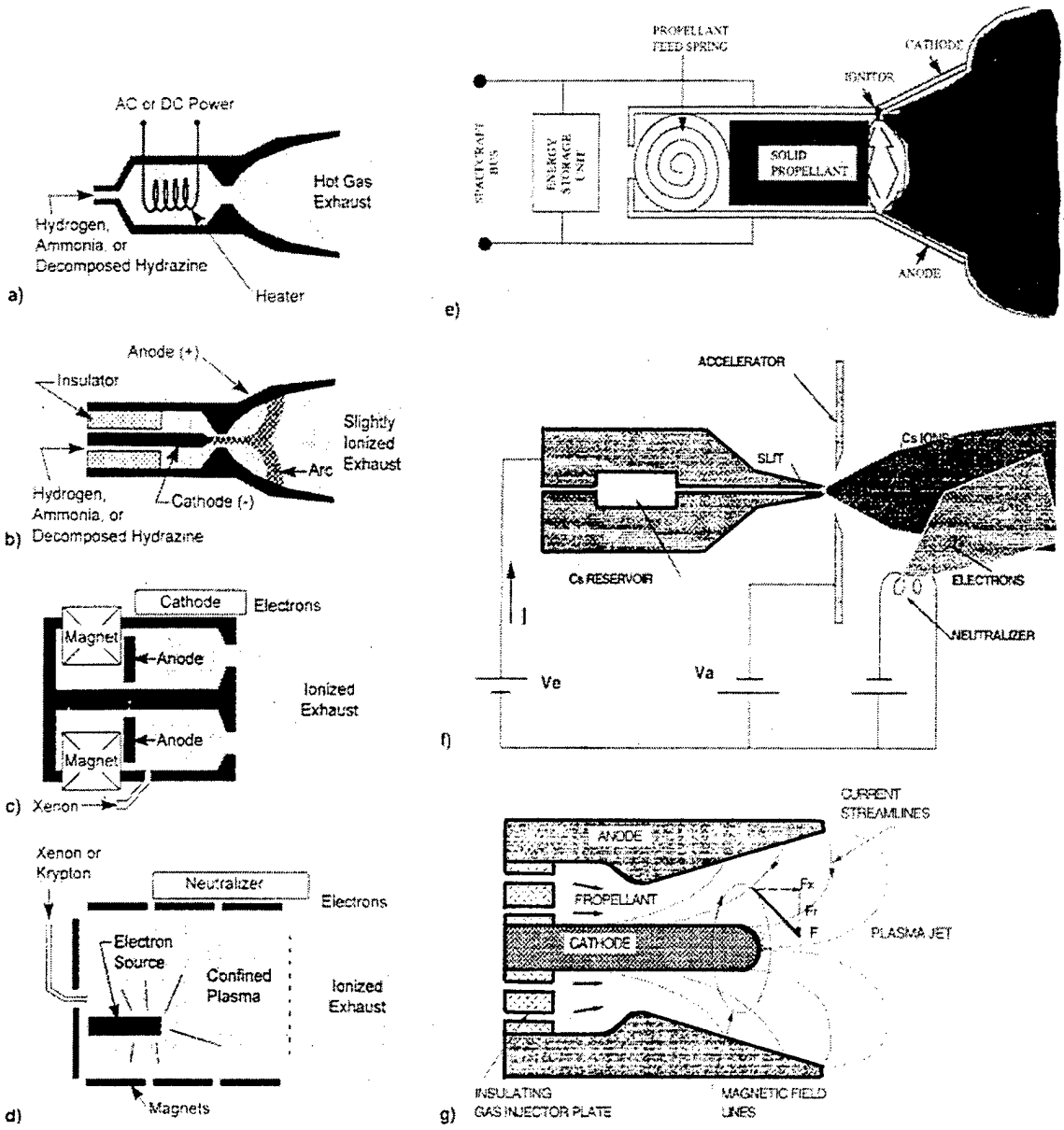

Figure 1. Operating Principles of Various Electrical Propulsion Thrusters.

From Martinez-Sanchez and Pollard, page 691.

(a) resistojets

(b) arcjets

(c) Hall thrusters

(d) ion engines

(e) pulsed plasma thrusters

(f) field-effect electrostatic propulsion thrusters

(g) self-field magnetoplasmadynamic thrusters

II. THEORETICAL BACKGROUND

A. FIRST PRINCIPLES

Electrical propulsion systems have four general yet unique characteristics. These characteristics are exploited in analyzing and understanding the electric propulsion system, and they are delineated in the following paragraph.

Electric propulsion engines (1) incorporate a comparatively heavy mass of required power generation equipment, and they (2) produce low thrust. As a result of that low thrust, (3) very low accelerations (on the order of 10^{-4} to 10^{-6} g_o) are attained (4) requiring long operating times. In the following development of the equations governing electrical engines, the electrical rocket's performance will be characterized in terms of power and mass as first proposed by Langmuir and Irving. (Sutton, 1992, pg. 596)

First, the mass aspects of electrical propulsion will be analyzed.

The major components integral to an electrically powered space vehicle are broken down as follows:

$$m_o = m_p + m_{pl} + m_{pp}. \quad (1)$$

In words, this equation states that the initial total mass of the vehicle (m_o) is equivalent to the sum of the masses of the propellant (m_p), payload (m_{pl}), and powerplant (m_{pp}). Refer to the list of symbols and abbreviations (on page xiii) for the comprehensive table of the following abbreviations and their respective units.

The determination of m_{pp} for an assigned mission is the most amorphous. This term incorporates a wide variety of components that make up the empty (or un-fueled) propulsion system. Those components include the thruster, the propulsion storage and

feed system, the energy source with its conversion system and auxiliaries as well as the associated structure (Sutton, 1992, pg. 597).

Now, let us look at the power aspects.

Regardless of the energy source (battery, nuclear, solar, fuel cells, etc.) to the input power supply, the input energy must always be greater than the required electrical power output, and power conversion efficiencies typically average approximately 70 percent. This aspect is accounted for in the engine parameter known as specific power, α, or the "state-of-the-art." It is defined as the ratio of electrical power output to the mass of the power plant, and it serves as an indication of the system's ability to effectively and efficiently generate or convert to electrical power. The equation for α is defined as follows:

$$\alpha = P_e / m_{pp}, \tag{2}$$

where P_e is the electrical power that is actually supplied to the propulsion system. Typical high "alpha" values that are currently attainable range from approximately 100 to 200 W/kg. It is a singular goal in electrical propulsion to strive to push this number to the highest attainable values. (Sutton, 1992, pg. 597)

In an electrical propulsion thruster, the electrical power input is converted to the kinetic energy of the propellant exhaust. Thus, P_e can also be defined by accounting for losses due to thruster efficiency, η_t, where

$$\eta_t = P_{jet} / P_e = (1/2)\ \dot{m}\ v^2 / P_e \text{ (Sutton, 1992, pg. 571)}, \tag{3}$$

and, consequently, we may redefine P_e as the following:

$$P_e = \alpha\ m_{pp} = (1/2)\ \dot{m}\ v^2 / \eta_t = m_p\ v^2 / (2\ t_p\ \eta_t). \tag{4}$$

In this equation, $\dot{m}$ is the propellant mass flow rate, v is the effective exhaust velocity, and t_p is the duration of operation in which the propellant mass, m_p, is ejected from the thruster. It is important to note that this equation assumes a *uniform rate* of propellant expulsion. (Sutton, 1992, pg. 597)

Using the previous definitions of m_o, α, and P_e, we can form the equation for the payload mass fraction, which is written,

$$m_{pl} / m_o = (1 - (v^2/(2 \alpha t_p \eta_t))(e^{\Delta u/v} - 1))/ e^{\Delta u/v}. \quad (5)$$

This equation assumes gravity-free and drag-free flight. Additionally, by defining the characteristic velocity, v_c, as

$$v_c^2 = 2 \alpha t_p \eta_t, \quad (6)$$

we can re-write the payload mass fraction as follows:

$$m_{pl} / m_o = (1 - (v / v_c)^2(e^{\Delta u/v} - 1))/ e^{\Delta u/v}. \quad (7)$$

In this form, the payload mass fraction is more manageable. (Sutton, 1992, pg. 597)

A plot of this equation is illustrated in Figure 2. The equation is graphed over the range of v / v_c for various values of $\Delta u / v_c$. It is evident that a maximum exists such that the payload mass ratio, m_{pl} / m_o, for a given velocity increment, $\Delta u / v_c$, is maximum at a particular value of exhaust velocity, v / v_c, or specific impulse, I_s / v_c. Specific impulse and effective exhaust velocity are related via the equation,

$$I_s = v / g_o \text{ where } g_o = 9.81 \text{ m} / \text{s}^2. \text{ (Sutton, 1992, pg. 597)} \quad (8)$$

The maximum described in these curves exists for two reasons. First, the inert mass of the power plant, m_{pp}, increases almost linearly with the specific impulse. However, the mass of consumed propellant decreases with specific impulse. The vehicle velocity increment, Δu, increases with higher I_s; however, Δu is also decreased by the

lower mass ratio due to the increased inert mass. Consequently, there is a unique optimum value of I_s (or v) for every electric propulsion mission as defined by the corresponding required value of Δu. (Sutton, 1992, pg. 597)

Again, refer to Table 1 for a brief summary of various mission Δu values.

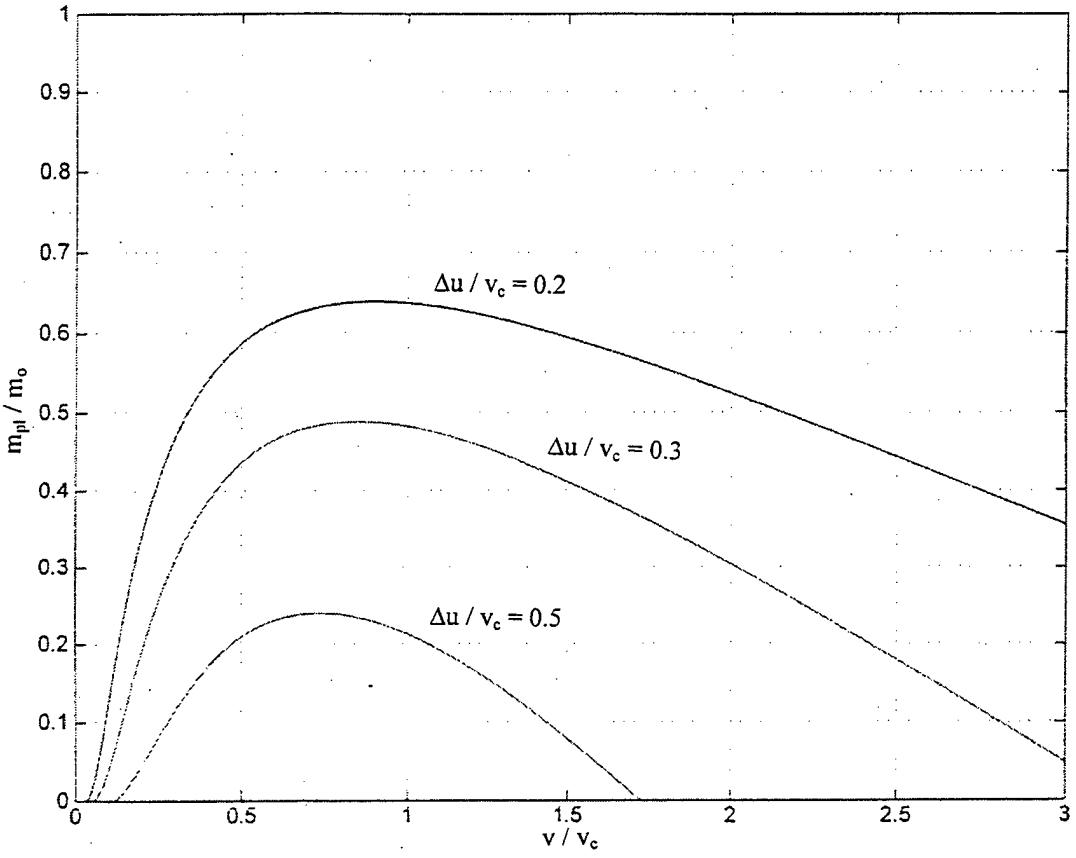

Figure 2. Payload Mass Fraction Plot: m_{pl} / m_o vs. v / v_c.

The payload mass ratio can also be re-written to a somewhat more useful form by solving for $\Delta u / v_c$. In this case, the equation takes on the following form:

$$\Delta u / v_c = (v / v_c) \ln [(1 + (v / v_c)^2)/((m_{pl} / m_o) + (v / v_c)^2)], \quad (9)$$

and it is plotted in Figure 3. In this case, the equation is graphed over the same range of

v / v_c for various values of m_{pl} / m_o.

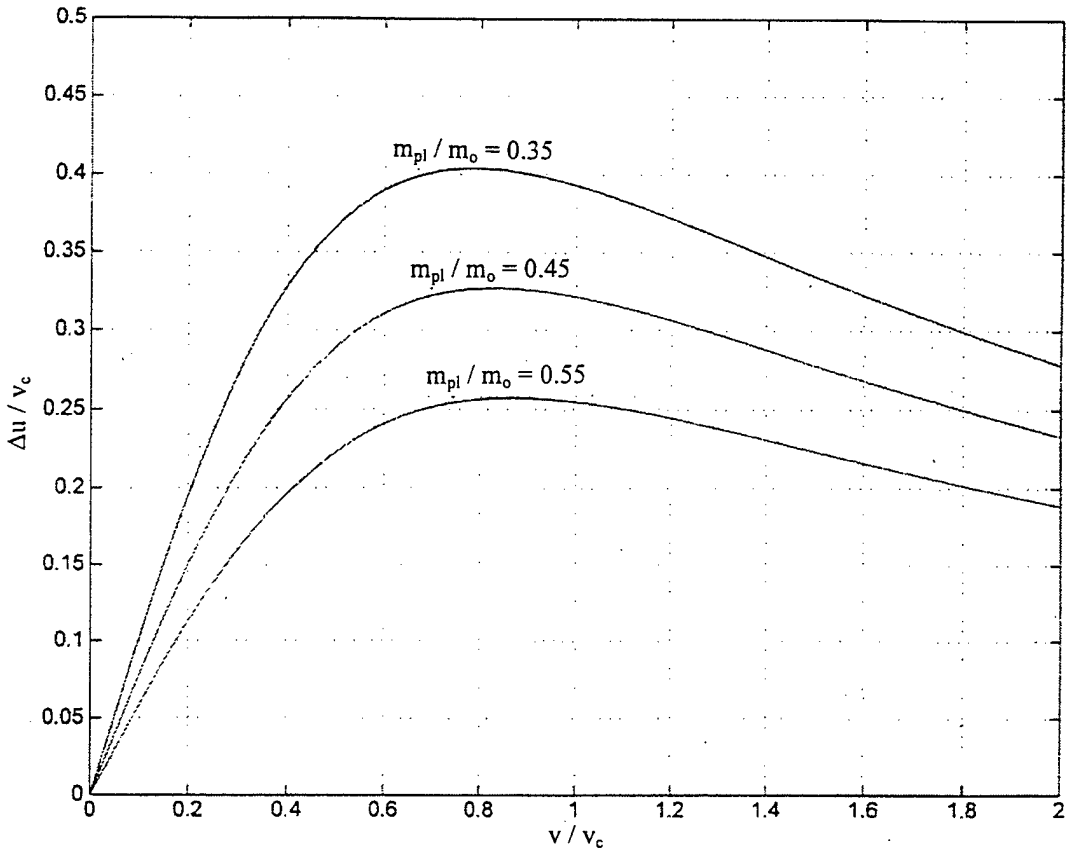

Figure 3. Payload Mass Fraction Plot: $\Delta u / v_c$ vs. v / v_c.

This graph shows the optimum curves for three different mass payload ratios. From this plot and the defining equations, we note that the optimal values for $\Delta u / v_c$ and v / v_c are as follows:

m_{pl} / m_o	$\Delta u / v_c \mid opt$	$v / v_c \mid opt$
0.35	0.404	0.782
0.45	0.327	0.820
0.55	0.257	0.864

Table 3. Optimum Values: $\Delta u / v_c$ and v / v_c for Various Payload Mass Ratios.

These values will be an essential aspect of our engine selection (or engine-mission matching) algorithm, which is developed in Chapter IV.

B. ANALYSIS – DUAL OPTIMUM METHODOLOGY

Incorporating the previous development via "first principles," it is now advantageous to establish a "joint" or "dual" optimum, which will optimizes the payload mass ratio and yields the minimum transfer time. It can be calculated by multiplying the payload mass ratio and the previously defined equation for $\Delta u / v_c$.

The plot of the resulting equation (for various payload ratios) is illustrated in Figure 4, and it shows that the dual-optimum payload mass ratio peaks at a value of $m_{pl} / m_o = 0.45$.

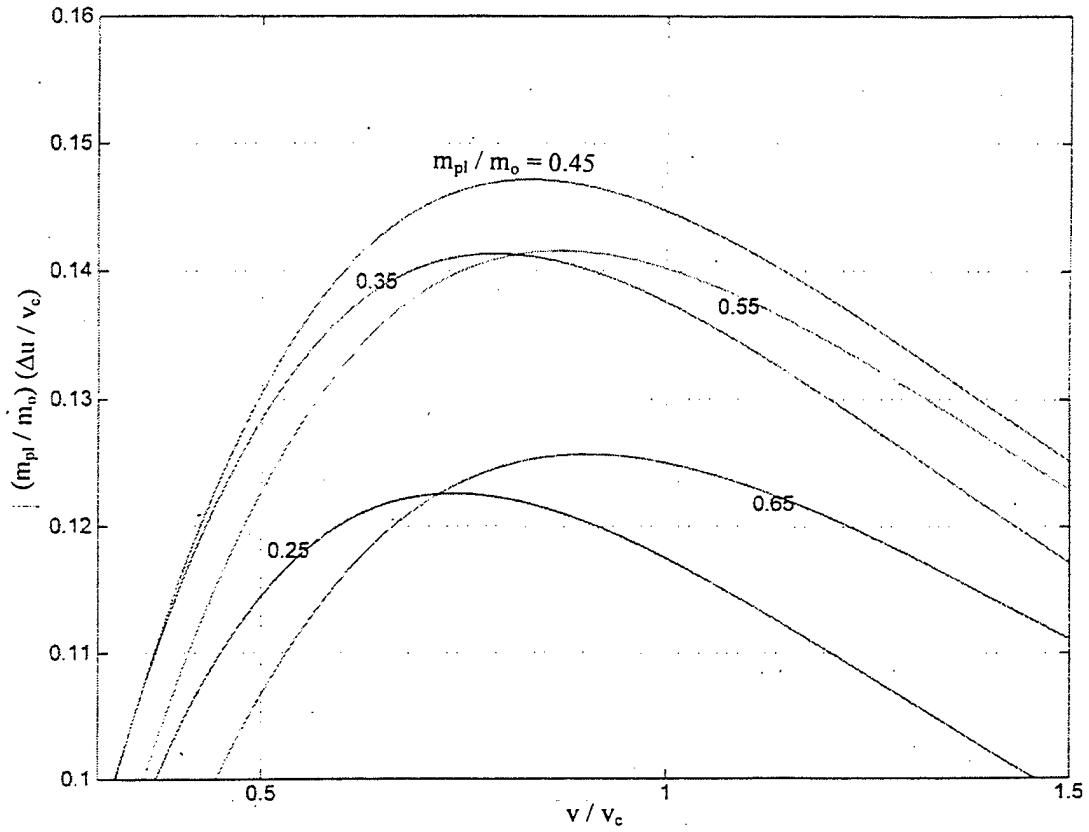

Figure 4. Dual Optimum.

This plot indicates that the optimum payload ratio is 0.45. However, due to the fact that it may be difficult for the designer to achieve this mass ratio, an approximate design range of payload mass ratios of 0.35 to 0.55 is investigated. As illustrated in Figure 4, these values do not lie too far below the optimum for 0.45.

It should be restated that for constant propellant mass flow ($\dot{m}$) constant thrust (F) and negligibly short start and stop transients:

$$I_s = F / \dot{m}\ g_o \text{ and } \therefore F = \dot{m}\ g_o\ I_s. \tag{10}$$

Hence, for a higher specific impulse, I_s, less fuel is required. However, as the specific impulse is increased, we may drive through the optimum due to the equation for $\Delta u / v_c$, which incorporates the applicable "efficiencies" of the engines in the forms of α, t_p, and η_t. As a result, an engine with an arbitrarily high I_s may not be optimum for a particular application or mission. For example, the Teflon PPT has relatively high values for I_s at the expense of comparatively poor values for α and η_t.

Figure 5 illustrates a three-dimensional optimum surface. The plot is illustrated across the axis values of...

x: v / v_c	range: 0.5 to 1.3
y: m_{pl} / m_o	range: 0.3 to 0.6
z: $(m_{pl} / m_o)(\Delta u / v_c)$	range: 0.115 to maximum at 0.148

The plot clearly shows the establishment of a optimum or maximum point at the payload mass ratio of precisely $m_{pl} / m_o = 0.45$.

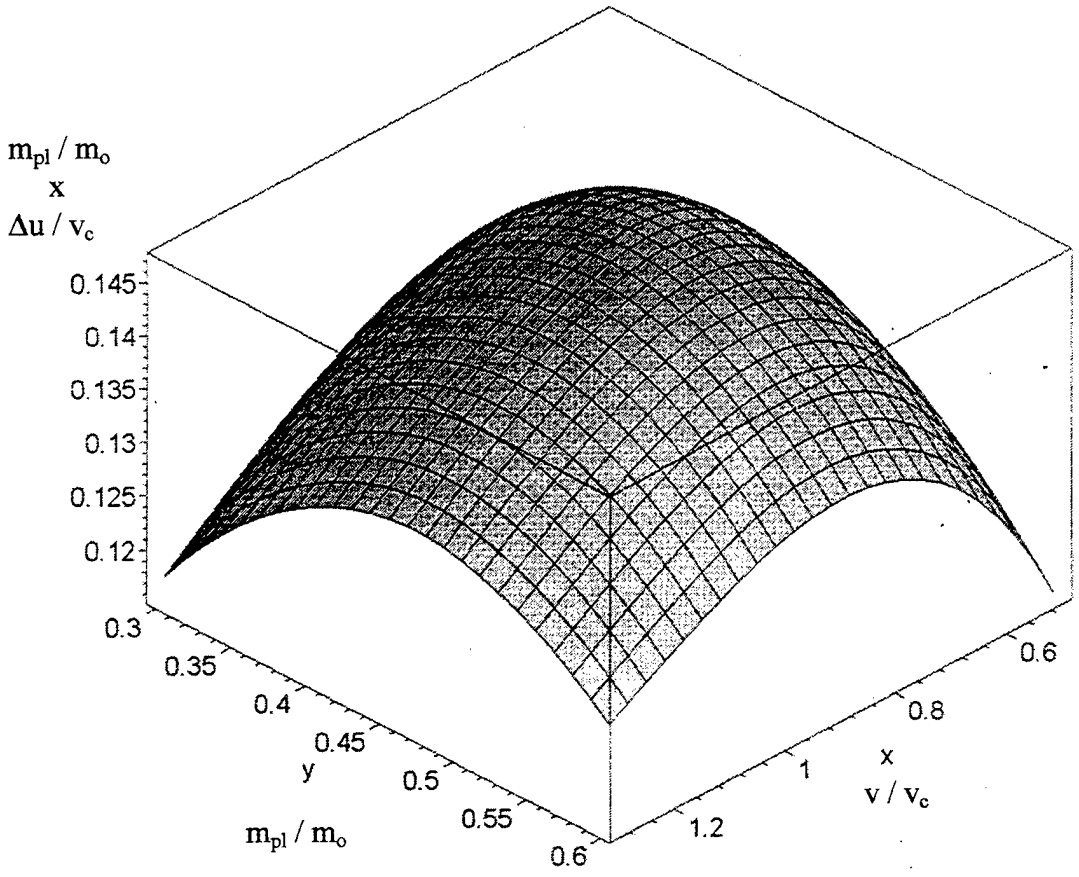

Figure 5. Three-dimensional Dual Optimum Surface.

C. TANKAGE PENALTY

The parametric curves that have been presented up to this point are inherently ideal in nature. They generally assume that all spacecraft mass can fall neatly into the three categories of mass of propellant, payload, or power-plant. However, as previously noted, it can be difficult to assess where exactly certain masses (such as shared power conditioning equipment) should be charged, and as a result, the calculation of the specific power, α, for the respective electric propulsion engine can have high variability. In the

same manner, one can assess somewhat of a "tankage penalty" in proportion to the amount of propellant required as a result of the following reasoning.

The typical propellant tanks are composed of overwrapped titanium or aluminum. Their loading varies depending upon several factors including satellite mass, expected life on orbit, mission (orbit raising, NSSK, etc.) and cant angle of thruster. As a result, the actual size and mass of tanks will vary regardless of engine type or manufacturer.

An accurate figure of merit for the required tankage revolves around the following assumptions. First, that a propellant tank that holds zero propellant mass is assessed at one kilogram. Second, that the tank has a mass fraction of approximately ten percent as a function of loaded propellant. It is important to note that all of the listed electrical propulsion engines, except the pulsed MPD type, require tankage. (Clauss, 1999)

For example, a tank that holds 40 kg of xenon would have a dry mass of...

1.0 kg + 0.1 (40 kg) = 5 kg.

If this 10 % tankage "penalty" and one kilogram of dead dry mass are incorporated into the previous analysis, the equation for the initial mass and components is altered from $m_o = m_p + m_{pl} + m_{pp}$ to $m_o = 1.1\ m_p + m_{pl} + m_{pp}$. However, the equation for final mass remains unaltered as follows: $m_f = m_o - m_p$. The $0.1\ m_p$ is residual mass that remains within the system.

Using these definitions, the equation for the rewritten payload mass ratio, solved for $\Delta u / v_c$, takes the following form:

$$\Delta u / v_c = (v / v_c) \ln [(1.1 + (v / v_c)^2)/((m_{pl} / m_o) + (v / v_c)^2 + 0.1)]. \qquad (11)$$

This equation is plotted as $\Delta u / v_c$ vs. v / v_c in Figure 6.

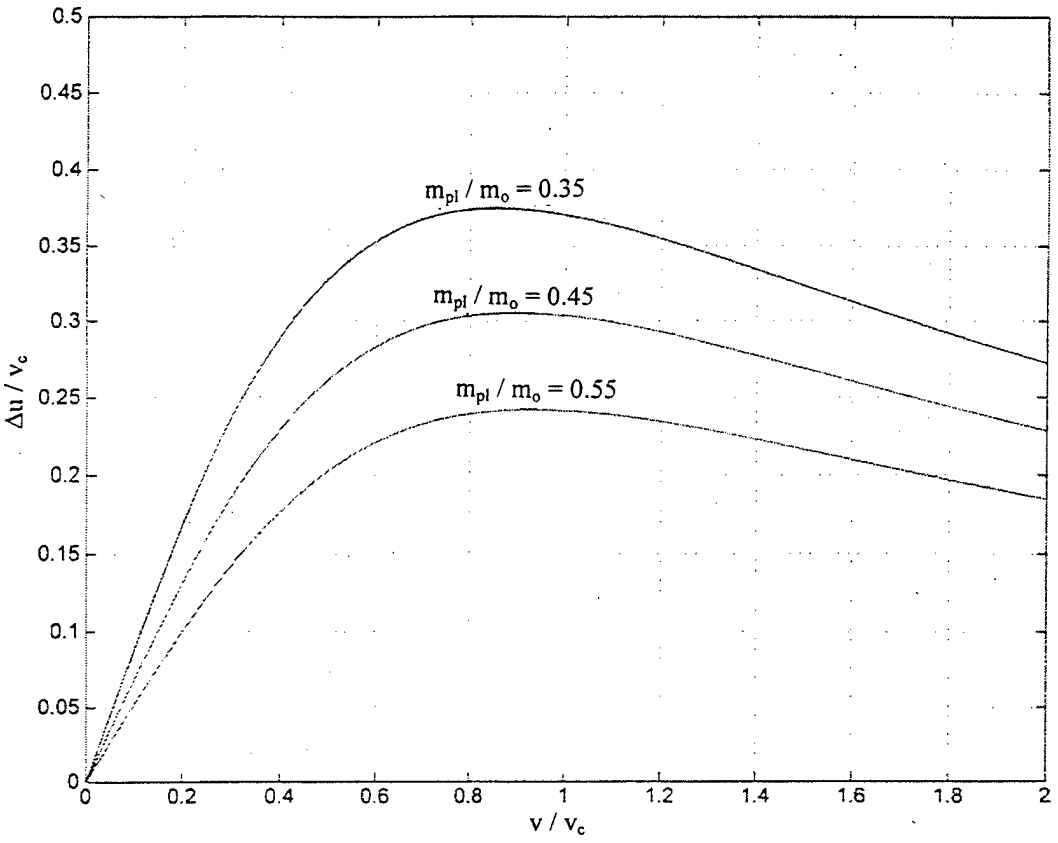

Figure 6. Payload Mass Fraction Plot with 10 % Tankage Penalty:

$\Delta u / v_c$ vs. v / v_c.

Note that the curve is essentially similar to the plot illustrated in Figure 3; however, it is adjusted for the ten percent tankage "penalty." As a result, the optimum curves have shifted down and right from their original values. This is illustrated in Figure 7 which shows the optimum curves with and without the tankage "penalty" for the payload mass ratio (m_{pl} / m_o) of 0.45.

For a ten percent tankage "penalty," the following optimal values for $\Delta u / v_c$ and v / v_c result:

m_{pl}/m_o	$\Delta u / v_c \mid opt$	$v / v_c \mid opt$
0.35	0.375	0.850
0.45	0.306	0.895
0.55	0.240	0.945

Table 4. Optimal Values with 10% Tankage Penalty: $\Delta u / v_c$ and v / v_c.

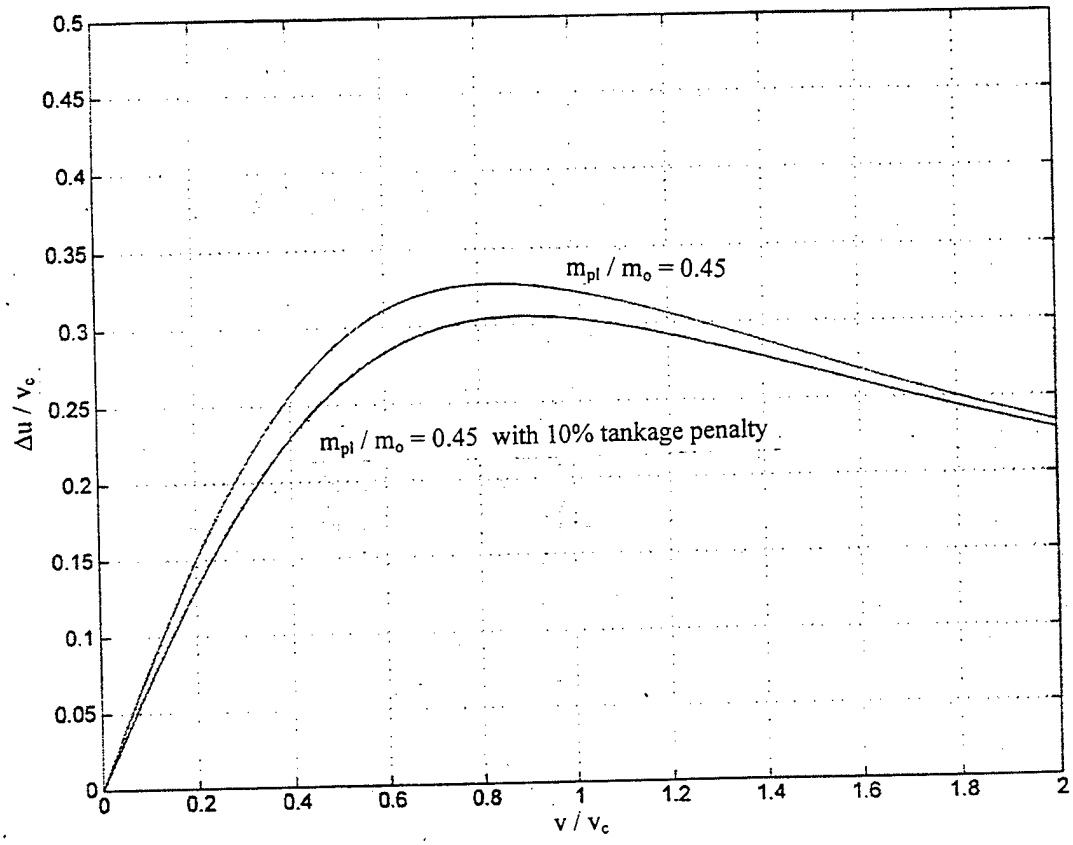

Figure 7. Optimum Comparison with and without 10 % Tankage Penalty:

$\Delta u / v_c$ vs. v / v_c at $m_{pl} / m_o = 0.45$.

For all of the plotted "tankage" penalty curves, the values plotted are for a 10 % penalty. Typical tankage fractions range from 0.05 for the hydrazine (N_2H_4) resistojet and arcjet to 0.15 for the H_2 arcjet. Xenon Hall thrusters and ion thrusters have tankage fractions of about 0.12. (Martinez-Sanchez and Pollard, 1998, pg. 690)

THIS PAGE INTENTIONALLY LEFT BLANK.

III. CURRENT TECHNOLOGY -- ELECTRIC ENGINES

A. NASA DEVELOPMENT AND OBJECTIVES

Today, there are many organizations pursuing the research and development of space electric propulsion. Various private companies (including Primex, Hughes, ARC, and Daimler Chrysler) presently offer electric propulsion engines for sale and use in various applications. Additionally, several research facilities -- such as NRL (Naval Research Labs) and NASA's JPL (Jet Propulsion Labs) -- have also developed various engines or components of engines. However, the one department of NASA that is primarily responsible for electric propulsion research is the On-board Propulsion Branch.

NASA's On-board Propulsion Branch is based at the John H. Glenn Research Center located on Lewis Field in Cleveland, Ohio. The branch is responsible for developing advanced on-board spacecraft propulsion technologies -- both chemical and electrical -- for future NASA missions. The electrical propulsion technologies currently under investigation at Lewis Field include resistojets, arcjets, gridded ion xenon thrusters, Hall xenon ion thrusters, and pulsed plasma thrusters (PPT's). (Oleson, 1999)

In October of 1998, the on-board propulsion branch celebrated two major milestones in the realm of electrical propulsion. Deep Space One (DS1) was successfully launched on October 24, 1998 from Florida's Cape Canaveral Air Station. This craft is intended to validate new space technologies, including its ion propulsion primary engine, which was developed in the NSTAR (NASA Solar Electric Propulsion Technology Application Readiness) program. NASA Glenn developed the engine and power processors for DS1, and this flight was the first-ever application of such a technology to a

deep space mission. DS1 was to rendezvous with the near-Earth asteroid, 1992 KD, in July 1999, and it passed within 15 miles of the asteroid Braille on July 28 at a speed of greater than 35,000 mph (15.5 km/s). (Oleson, 1999)

DS1's NSTAR ion engine utilizes 81 kilograms of xenon propellant, which it ionizes and accelerates to 68,000 mph. The engine, which is 12 inches in diameter, can operate at half throttle for greater than 20 months, generating a continuous thrust of 0.02 lbf. As a result, the engine is ten-times more fuel efficient than a comparable chemical system, and it is the prototype for smaller / lower-cost space vehicles. (Oleson, 1999)

On October 3, 1998, a STEX spacecraft was launched, carrying the EPDM (Electric Propulsion Demonstration Module). This module was developed under joint effort on the part of NASA, Naval Research Labs (NRL) and private industry. The Glenn Research Center led the program, which was intended to demonstrate the first use of a high specific impulse, low-power Hall thruster system on a U. S. spacecraft. (Oleson, 1999)

That particular Hall engine is a TAL (Thruster with Anode Layer) D-55 Hall-effect thruster. It was developed by the Russian Central Research Institute of Machine Building (TSNIIMASH), and it successfully operated, firing ten times from 23 to 24 October. The engine provided 40 mN of thrust and raised the satellite's orbit 0.35 NM. (Oleson, 1999)

As electrical propulsion evolves, NASA Glenn has clearly defined its objectives.

For fiscal year 1999, four major product targets have been defined. Those targets include a next generation ion system for near- and further-term space science and a

pulsed plasma thruster (PPT) technology for precision imaging. In addition, NASA would like to develop both a high specific impulse, low-mass Hall system and a miniature electrothermal thruster for Earth science. (Oleson, 1999)

NASA Glenn has also defined what it calls "grand challenges" in the development of electrical propulsion. Those challenges are delineated for each of the three types of electrical propulsion systems, and they are outlined as follows: (Oleson, 1999)

Electrothermal Thrusters:

- integrated electronics / thruster package for micro-spacecraft applications

Electrostatic Thrusters:

- lightweight, high total impulse ion systems for space science
- very high total impulse ion system for far-term space science

Electromagnetic Thrusters:

- low-cost, simple, low-power Hall for miniature Earth-orbital spacecraft
- high specific impulse (I_s), direct drive Hall for space science and Earth orbital
- increase thruster efficiency by factor of two to 16%
- increase capacitor life to 40,000,000 pulses and beyond
- lower electromagnetic emissions to below present standard specifications
- predict contamination on spacecraft surfaces in design phase

Nonetheless, the ability and timeliness of electric propulsion to meet these challenges is unpredictable. This is due inherently to the fact that the "state of the art" in electric propulsion is due and determined largely by the "state of the art" of the electrical components that comprise various aspects of the electrical propulsion system. Primarily, the concern is the required additional mass of electrical components. This fact will

become evident in the forthcoming discussion of the specific power or "alpha" (α) parameter.

B. SUMMARY OF AVAILABLE ENGINE DATA

One of the contributions of this thesis is to obtain and summarize the most current reported data regarding present-day electric propulsion engine performance characteristics. This summary, which includes data from various vendors as well as the above research sites, can be found on page 36 in Table 5: Summary of Current Technology Engines, and the various sources of this information are listed at the bottom of the table. Figure 8, on page 35, provides an overall map of current engines and their respective values of specific impulse, I_s.

The electrical engine parameter that has certainly been the most difficult to define has been an accurate representation of the parameter α, specific power or "state of the art." This parameter is so named because it defines the relation of the power conversion unit with respect to the system's mass. In other words, as previously defined, $\alpha = P_e / m_{pp}$, where P_e is the power supplied to the electrical propulsion system and m_{pp} is the power-plant mass (Sutton, 1992, pg. 597).

The apparent controversy surrounding the "state of the art" parameter is evidenced in the article "Optimization of Electric Propulsion Systems Considering Specific Power as Function of Specific Impulse" by M. Auweter-Kurtz et al. This article, found in the Nov.-Dec. 1988 issue of the AIAA *Journal of Propulsion and Power*, presents the argument that specific power, α, is a strong function of specific impulse, I_s, or exhaust velocity, v. Specific impulse and exhaust velocity are related via the equation, $v = I_s g_o$.

The article notes that several different organizations have conducted optimizations for various missions and that those optimizations assumed a *constant* specific power of the propulsion system. This assumption is arguably a potential source of error in that it implies the following about variations in power levels and specific impulse. First, it assumes that constant thrust and system efficiency could be evident with a changing specific impulse. Additionally, it implies that constant specific power could be maintained with changing power levels during optimization. (Auweter-Kurtz et. al., 1988, pg. 512)

In undertaking this optimization analysis, this point was certainly considered. However, due to the fact that the trace of an engine's efficiency is not continuous, average values were utilized over limited specific impulse ranges thereby assuming no strong dependence on specific impulse or exhaust velocity.

Still, it is not elementary to assign α values to a particular engine.

Items of concern in determining specific power include such things as the number of engines that will be necessary for a specific mission and whether or not those same engines can share various components of the power conditioning equipment. If power conditioning components can be shared, then α improves as mass is decreased. Likewise, α would be detrimentally affected if more mass were required such as additional solar cell panels to power required thrusters.

Specific power also can be improved if the electrical propulsion system can be powered through the systems already integral to the payload. As such, the question arises as to where that mass should be billed. If it is attributed to the payload mass (m_{pl}), then again the value for specific power is improved.

In summary of the above concerns, it should be evident that the α parameter is not only engine specific but also configuration (number of engines and shared components or redundancy) and design (payload compatible power sources) specific.

In order to demonstrate this aspect of the determination of the value for specific power, the following example is illustrated.

Atlantic Research Corporation is one of the current suppliers of one of the commercially available Hall-type thrusters. In their brochure for the SPT-100, they depict the configuration for a "typical SPT-100 propulsion system for GEO satellites."

The system depicted consists of the following major components: four SPT-100 thrusters, four pairs of xenon flow controllers (XFC's), two PPU-100 power processing units, the propellant management assembly (PMA), and two xenon storage tanks. The entire configuration allows for redundancy; therefore, we would assume that the designed mission would require the use of only two of the four thrusters. (ARC brochure, 1998)

In determining specific power, it is necessary to account for the masses of all components that encompass the power-plant mass (m_{pp}). This does not include the actual mass of the propellant (m_p). Thus, it is often referred to as the "dry mass" -- probably hailing from the early days of liquid rocket propulsion.

The masses of all of the components are as follows:

SPT-100 (4).....3.5 kg / SPT

XFC (4 pairs).....0.64 kg / pair

PPU-100 (2).....6.2 kg / PPU

PMA.....3.25 kg

However, the mass of the xenon tanks is mission dependent. (Clauss, 1999)

The tank mass can be estimated in the manner demonstrated in Chapter II, C. Again, assuming that a tank which holds zero propellant mass weighs 1 kg and that the tank has a mass fraction of 0.1 to 0.12 (as a function of the mass of xenon), then for a 40 kg of xenon, a 5 kg tank should be required as 1 kg + (0.1)(40 kg) = 5 kg. (Clauss, 1999)

In the brochure example for a GEO satellite, we pick a usable example of a 15-year GEO satellite for NSSK. Such a mission would require approximately 120 kg of xenon to be held in two tanks. Hence, 60 kg of xenon would be held in each tank. Accordingly, one tank would then weigh 7 kg as 1 kg + (0.1)(60 kg) = 7 kg.

Nowhere in any current publications is there a discussion as to how to "charge" mass values in determining specific power or "alpha." In this case, all "dead" mass is attributed to power-plant mass (m_{pp}), and all mass that is proportional to power is assigned to payload mass (m_{pl}). Hence, we would have to include 2 kg of tankage in our value for power-plant mass.

With the value for tank mass, it is now possible to calculate the power-plant mass as follows:

$m_{pp} = 4\ (3.5\ kg)_{SPT} + 4\ (0.64\ kg)_{XFC} + 2\ (6.2\ kg)_{PPU} + 3.25\ kg_{\ PMA} + 2.0\ kg_{\ tanks}$.

Thus, $m_{pp} = 34.2$ kg.

Each of the SPT-100 thrusters requires 1.35 kW of power delivered at 300 V and 4.5 A. With a known PPU efficiency of $\eta_{PPU} = 0.93$, we are able to calculate that a total of 5,808 W must be delivered to the thruster bank. Hence, we are now able to calculate the specific power for the configuration. (Clauss, 1999)

$\alpha = P_e / m_{pp} = 5{,}808\ W / 34.2\ kg = 169.8\ W/kg.$

It can not be overemphasized that this calculated value of specific power for the SPT-100 is only for the illustrated four-thruster configuration as designed for the mission of a 15-year GEO satellite. Otherwise, the masses change, and specific power must be re-calculated.

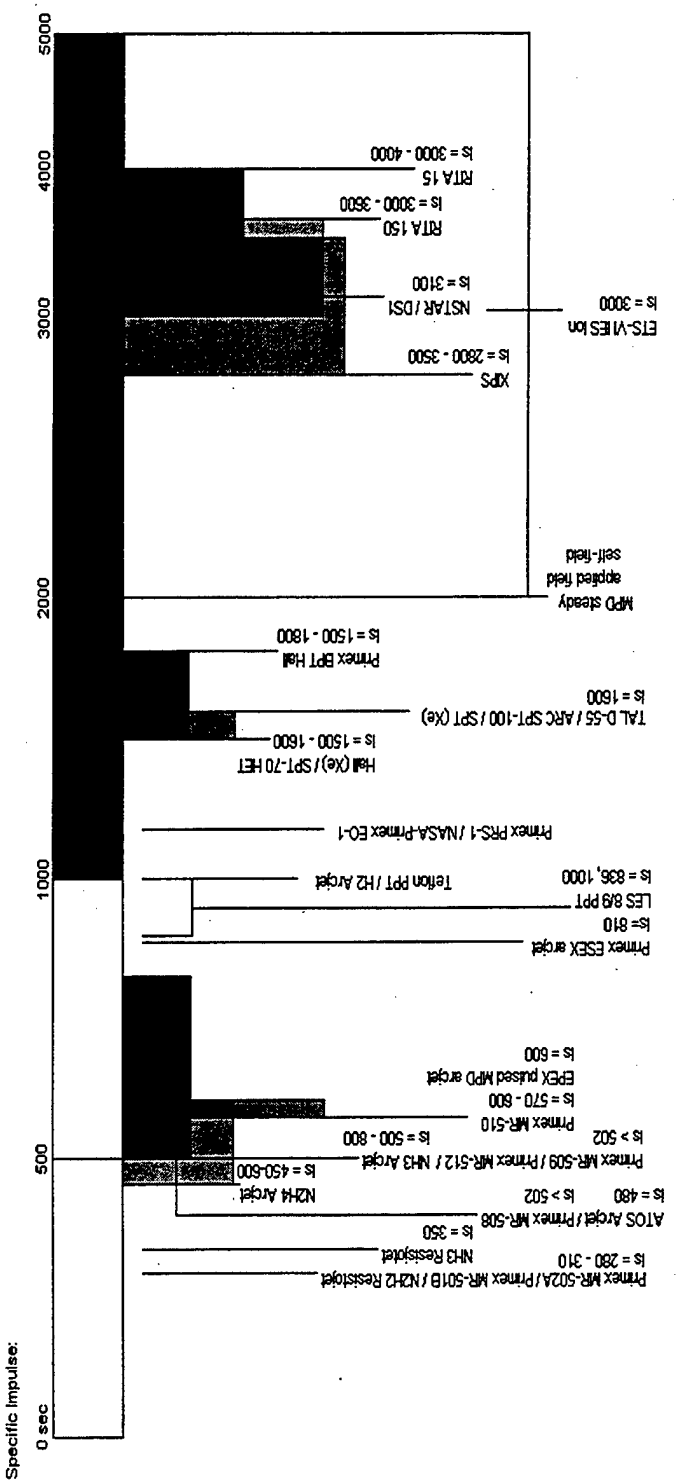

Figure 8: Specific Impulse (I_s) Ranges for Current Technology Engines

ENGINES(source)	alpha (W/kg)	nt	Is (sec)	Pinput(W)	thrust (N)	lifetime (hrs)	status
RESISTOJET							
N2H4 (1,2)	333 - 500	0.8 - 0.9	280 - 310	500 - 1500	0.2 - 0.8	> 390	operational
NH3 (2)		0.8	350	500			
Primex MR-501B (8,10)			303 - 294	350 - 510	0.369 - 0.182	> 389	operational
Primex MR-502A (8,10)			299 nom.	610 - 885	0.80 - 0.36	> 370	operational
ARCJET							
N2H4 (1)	313	0.33 - 0.35	450 - 600	300 - 2000	0.2 - 0.25	> 830 - 1000	operational
H2 (1,2)	333	0.4	1000	5 - 100 K	0.2 - 0.25	>1000	lab
NH3 (2)	270 - 320	0.27 - 0.36	500 - 800	500 -30 K	0.2 - 0.25	1500	qualified
IRS ATOS (Ger) (10)		0.362	480	748	0.114	1,010	qualified
Primex MR-508 (5,10)		0.3	> 502	1800	0.200-0.231	> 830	operational
Primex MR-509 (8,10)	~ 115.3	> 0.31	> 502 (545)	1800	0.213 - 0.254	> 1575	qualified
Primex MR-510 (8,10)	~ 150	> 0.31	> 570 - 600	2170	0.222 - 0.258	> 2595	qualified
Primex MR-512 (8)	~ 103	> 0.91 (PCU)	> 502	1780	0.213 - 0.254	> 1575	in production
Primex ESEX (10)		27.2 +/- 1	810	26,000	1.8 - 2.0	1500	qualified
ION							
XIPS (1)	100	0.75	2800 - 3500	200 - 4000	0.015 - 0.04	> 8000	operational
Hughes XIPS-13 (10)		0.46, 0.513, 0.54	2585, 2720	427, 439	0.0178, 0.018	12,000	qualified
Hughes XIPS-25 (10)		0.65, 0.67	2800	1400	0.0635	> 4350	qualified
NSTAR/DS1 (5,7,10)	~ 45	0.6	3100	2300 - 2500	0.093	> 10,000	operational
Hughes HS601HP (9)			2568	500	0.018		
Hughes HS702 (9)			3800	4500	0.165		
RITA 15 (6)	~ 9.61		3000 - 4000	540	0.015	> 20,000	
RITA 150 (6)	~ 52.1		3000 - 3600	4300	0.15	> 20,000	
UK-10/T5 (UK) (10)		0.55 - 0.64	3090 - 3300	278 - 636	0.010 - 0.025	10,700	qualified
ETS-VI IES (Jap) (10)		0.4	3000	730	0.02		operational
DASA RIT-10 (Ger) (10)		0.38	3000, 3150	585	0.015		operational
HALL							
Hall (XE) (2,4)	150	0.5	1500 - 1600	300 - 6000	0.04	> 7000	operational
SPT (XE) (1)		0.48	1600	150 - 1500	0.04 - 0.2	> 4000	
ARC/Fakel SPT-100 (3,10)	~ 169.8*	0.48	1600	1350	0.083	> 7424	operational
Fakel SPT-70 (3)		0.46, 0.50	1510, 1600	640 - 660	0.04	9000	operational

Table 5: Summary of Current Technology Engines.

SPI T-40 (11)		0.40 - 0.45	1600 - 1630	150 - 210	0.008 - 0.011		lab
SPI T-140 (11)		> 0.55	1800 - 2100	2000 - 4000	0.200 - 0.210	8000	lab
SPI T-220 (11)		TBD	TBD	10K - 20K	TBD		development
T-100 SPT (10)		0.49, 0.52	1630	1350	0.083	> 8000	lab
TAL D-55 (Russia) (5,10)	~ 50.9	0.48, 0.50 - 0.60	1600, 950 -1950	600-1500	0.082	> 5000	operational
Primex BPT Hall (8)		0.5	1500 - 1800	500 - 6000			development
MPD -- steady							
applied field (2)		0.5	2000 - 5000	1 -100 K			lab
self-field (2)		0.3	2000 - 5000	200-4000 K			lab
MPD -- pulsed							
Teflon PPT (2)	1	0.07	1000	1 - 200	4000 N-s	>10^7 pulses	operational
LES 8/9 PPT (10)		0.0068, 0.009	836, 1000	25, 30	0.0003	>10^7 pulses	operational
NASA/Primex EO-1 (8)	~ 20	0.098	1150	up to 100	3000 N-s **		operational
Primex PRS-101 (8)			1150		1.4 mN, 2 Hz		operational
EPEX arcjet (Jap) (10)		0.16	600	430	0.023		operational
last update: 29 October 99							
SOURCES:							
(1) *Electric Propulsion for Spacecraft*, CPIA Bulletin / Vol. 22, No. 5, September 1996.							
(2) *Spacecraft Electric Propulsion -- An Overview,* Martinez-Sanchez, AIAA Journal of Propulsion and Power, Sept-Oct 1998.							
(3) ARC (Atlantic Research Group) portfolio re: Stationary Plasma Thruster.							
(4) News Briefs: "Navy's Hall Thruster Electric Propulsion System Goes Operational," *Space Tracks*; March/April 1999.							
(5) Mr. Mike Osborn of Naval Research Labs (mosborn@space.nrl.navy.mil).							
(6) brochure: "RITA -- The Ion Propulsion System for the Future," Daimler Chrysler Aerospace.							
(7) "Innovative Engines," *NASA Facts*; March 1999.							
(8) PRiMEX Aerospace "Space Systems Capabilities & Technologies" catalog 1997.							
(9) Hughes Space and Communications: "XIPS: The Latest Thrust in Propulsion Technology".....							
(10) *Electric Thruster Systems Enter 'Era of Application'*, CPIA Bulletin / Vol. 23, No. 5, September 1997							
(11) brochure: "Hall Effect Thrusters," Space Power, Incorporated							
NOTES:							
* alpha value calculated for 4 SPT-100 configuration as advertised for typical GEO satellites							
** additional data: thrust / mass = 250 micro-N / kg (1.4 mN at 2 Hz); fuel = 0.3 kg Teflon; PPE efficiency > 0.80							
~ = estimated parameter							

THIS PAGE INTENTIONALLY LEFT BLANK.

IV. PLANNING / OPTIMIZATION ALGORITHM – MATCHING THE MISSION, PAYLOAD, AND ENGINE

OPTIMUM DESIGN PROCEDURE:

1. Specify the Mission.

Define the mission profile in terms of the velocity requirements (Δu) and payload mass (m_{pl}). List additional constraints such as mission time (t_m), power (P_e), cost, etc.

2. Estimate the payload mass ratio, m_{pl} / m_o.

Based upon past operational and flight-test experience, an initial estimate of suitable candidate electric propulsion thrusters may yield an approximate expected payload mass ratio. Note: This initial "ballpark" estimate is primarily based upon mission profile (velocity requirement) and suitable engines, looking at cost, mission time, and operational flight experience.

In order to remain near the optimum for engine performance (as illustrated in earlier plots), a potential payload mass ratio range (from $m_{pl} = 0.35$ to 0.55) is selected with the corresponding numbers for $\Delta u / v_c$ and v / v_c.

IDEAL: without "tankage" penalty (i.e., particularly for Teflon PPT):

$m_{pl} / m_o = 0.35$: $\Delta u / v_c = 0.404$; $v / v_c = 0.782$.
$m_{pl} / m_o = 0.45$: $\Delta u / v_c = 0.327$; $v / v_c = 0.820$.
$m_{pl} / m_o = 0.55$: $\Delta u / v_c = 0.257$; $v / v_c = 0.864$.

"TANKAGE": with 10 % tankage penalty:

$m_{pl} / m_o = 0.35$: $\Delta u / v_c = 0.375$; $v / v_c = 0.850$.
$m_{pl} / m_o = 0.45$: $\Delta u / v_c = 0.306$; $v / v_c = 0.895$.
$m_{pl} / m_o = 0.55$: $\Delta u / v_c = 0.240$; $v / v_c = 0.945$.

If none of the listed payload ratios will suffice (or if further iteration shows that an intermediate value for payload ratio is appropriate), the required numbers for $\Delta u / v_c$ and v / v_c can be obtained from the plots in Figures 8 and 9. These graphs are for ideal systems and systems requiring "tankage" respectively.

3. Calculate the corresponding specific impulse, I_s, based upon payload mass ratio... using the tabular data below and the equation,

$$I_s = v / g_o.$$

IDEAL: without "tankage" penalty:

$m_{pl} / m_o = 0.35$: $I_s = 1.936\ \Delta u / g_o$.
$m_{pl} / m_o = 0.45$: $I_s = 2.51\ \Delta u / g_o$.
$m_{pl} / m_o = 0.55$: $I_s = 3.36\ \Delta u / g_o$, where $g_o = 9.81\ m / s^2$.

"TANKAGE": with 10 % tankage penalty:

$m_{pl} / m_o = 0.35$: $I_s = 2.27\ \Delta u / g_o$.
$m_{pl} / m_o = 0.45$: $I_s = 2.92\ \Delta u / g_o$.
$m_{pl} / m_o = 0.55$: $I_s = 3.94\ \Delta u / g_o$, where $g_o = 9.81\ m / s^2$.

For intermediate values of payload mass ratio, this same calculation can be accomplished using the ratios from Figures 8 and 9 along with the following equation,

$$I_s = (v / v_c) (v_c / \Delta u) (\Delta u / g_o).$$

4. Designate a candidate electric propulsion engine.

Referencing Figure 8 (on page 35), select the engine (or engines) whose available range of specific impulse, I_s, most closely matches the calculated value necessary for the optimum profile.

Engine selection also locks in the characteristic engine performance values for specific power (α), thruster efficiency (η_t), and available thrust. These values can be found in the comprehensive summary of Table 5 on pages 36 and 37.

Again, if no engine proves an adequate match for the calculated values of I_s, it is necessary to use the graphs depicted in Figures 9 and 10 and attempt intermediate values of mass payload ratio within the range.

5. Calculate burn time, t_p.

Determine the thruster burn time for the profile from the following formula,

$t_p = ((v_c / \Delta u)\, \Delta u)^2 / (2\ \alpha\ \eta_t)$.

At this point in the process, all of the above values are given: Δu from mission profile, $v_c / \Delta u$ from step 2, α and η_t from Table 5.

6. Check that burn time, t_p, is less than both mission time, t_m, as well as the design lifetime of the designated engine.

If burn time exceeds acceptable mission time or design life of the thruster, select another electric propulsion candidate (step 4) or vary the payload mass ratio (step 2).

7. Calculate the anticipated masses of the propellant (m_p) and power-plant (m_{pp}) via the following formulas for the respective payload mass ratios:

IDEAL: without "tankage" penalty (i.e., for Teflon PPT):

$m_{pl} / m_o = 0.35$: $\quad m_p = 1.152\ m_{pl}$; $m_{pp} = 0.612\ m_p$
$m_{pl} / m_o = 0.45$: $\quad m_p = 0.731\ m_{pl}$; $m_{pp} = 0.672\ m_p$
$m_{pl} / m_o = 0.55$: $\quad m_p = 0.469\ m_{pl}$; $m_{pp} = 0.746\ m_p$

"TANKAGE": with 10 % tankage penalty (i.e., for all other engines):

$m_{pl} / m_o = 0.35$: $\quad m_p = 1.078\ m_{pl}$; $m_{pp} = 0.723\ m_p$
$m_{pl} / m_o = 0.45$: $\quad m_p = 0.679\ m_{pl}$; $m_{pp} = 0.801\ m_p$
$m_{pl} / m_o = 0.55$: $\quad m_p = 0.432\ m_{pl}$; $m_{pp} = 0.893\ m_p$

For intermediate payload ratios, the following equations must be used...

(a) m_{pl} / m_o = desired ratio.
(b) $m_{pp} = (v / v_c)^2\ m_p$.
(c) $m_o = m_p + m_{pp} + m_{pl}$.
(d) m_{pl} is given.

8. Determine the total mass of the assembled vehicle (m_o) and verify the payload mass ratio.

$m_o = m_p + m_{pp} + m_{pl}$. mass ratio = m_{pl} / m_o.

9. Determine the required thrust based on the values for specific impulse, I_s, and propellant mass, m_p. Determine the required power to be delivered to the thruster.

$F = (m_p / t_p) I_s g_o$. $P_e = \alpha\ m_{pp}$.

Note: This calculated value of P_e should not greatly exceed the current "state of the art" for power generation (fuel cells, battery, or solar cells) of approximately 20 kW. If the power requirements cannot be met, return to step 4.

10. From the thrust calculation and the engine thrust characteristics (step 4), calculate the number of engines required to provide that thrust for the assigned mission.

11. Design check.

Considering component redundancy, is this design acceptable? That is, with current technology, is this a reasonable number of required engines? If not, return to design step 4 or attempt an intermediate payload ratio (step 2).

If yes, it may be advisable to iterate in order to account for redundancy thereby improving the α parameter. In other words, are there any components that the thrusters may be able to share, thereby reducing m_{pp} and improving α. This will improve overall performance by reducing mass and possibly reducing the number of engines required for the mission.

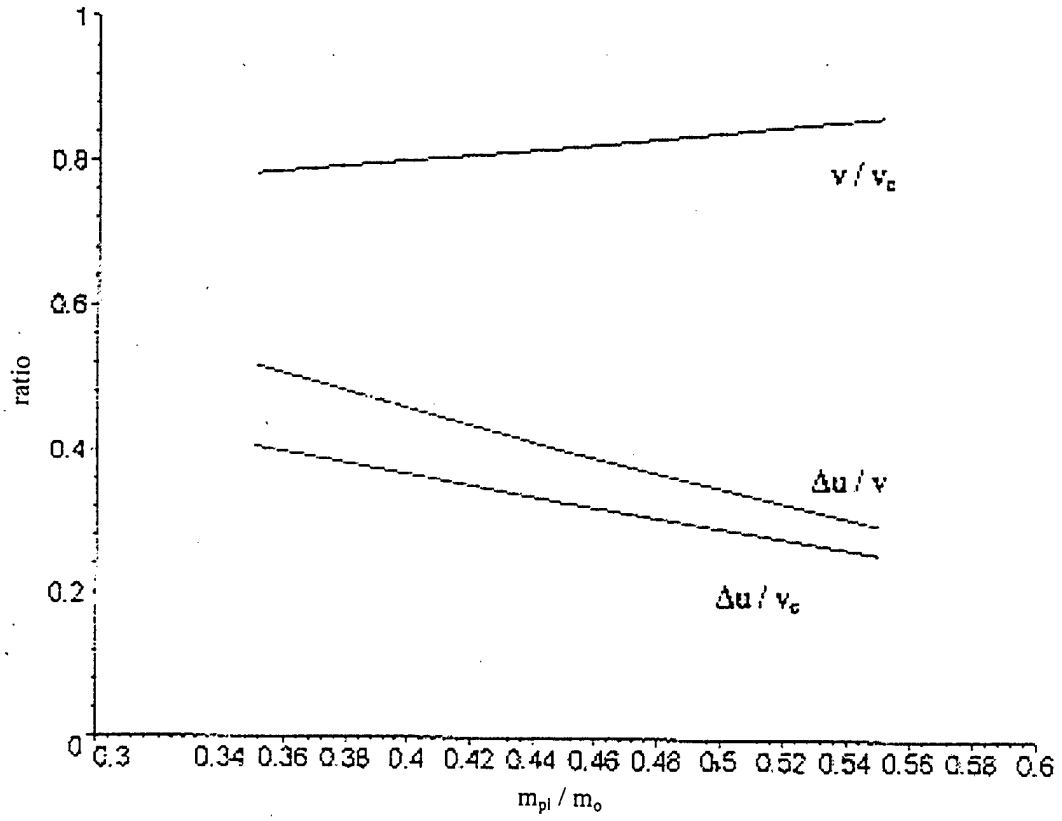

Figure 9: Comprehensive Plot of $\Delta u / v_c$ and v / v_c for Ideal Systems.

This plot serves as a baseline plot of the values of $\Delta u / v_c$ and v / v_c for all anticipated payload mass ratios between the optimum selection points of $m_{pl} / m_o = 0.35$ and 0.55. The points roughly bracket the optimum point at $m_{pl} / m_o = 0.45$.

This plot is usable only for ideal estimates of the calculations discussed in the design calculation, and it is usable for systems that do **not** require fuel tanks – i.e. no "tankage penalty." Such electric thrusters or engines include the pulsed MPD thrusters: Teflon PPT, LES 8/9 PPT, NASA Primex EO-1, and the Primex PRS-101.

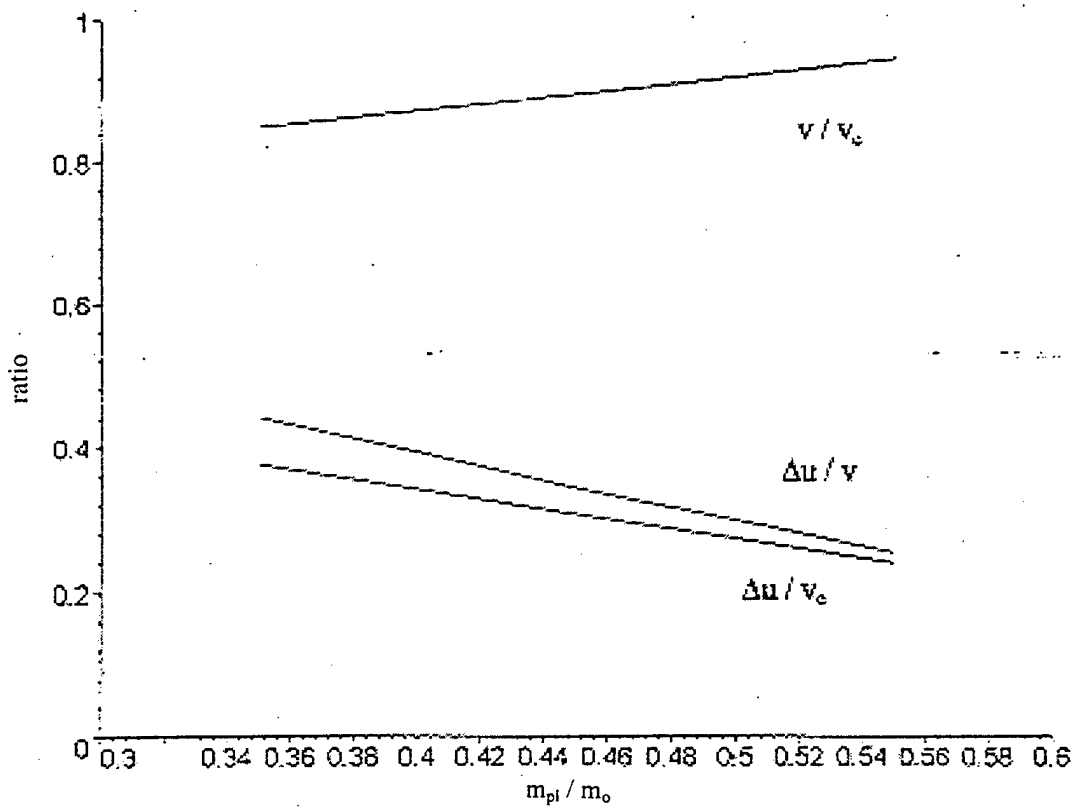

Figure 10: Comprehensive Plot of $\Delta u / v_c$ and v / v_c
for Systems Requiring "Tankage" of 10%.

This plot is acceptable for use with all electric propulsion thrusters that require fuel storage tanks. Therefore, it may be used for "tankage penalty" calculations for all of the engines listed except the pulsed MPD type.

Because of the fact that these plots take fuel tank considerations into account, this chart (or at least the determined values for the defined payload rations) should be consulted.

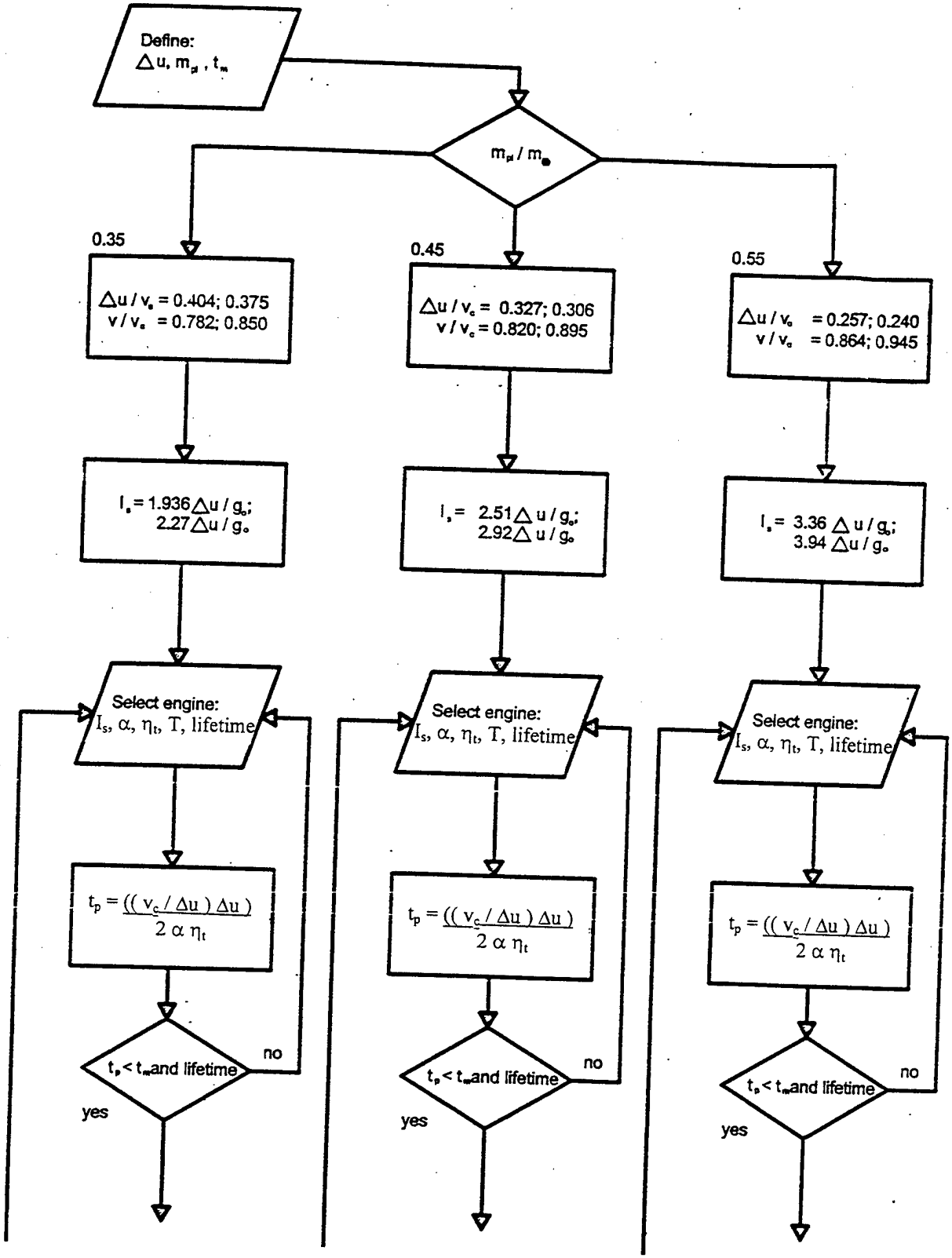

Figure 11: FLOWCHART -- Optimization Procedure for Electric Propulsion Engines

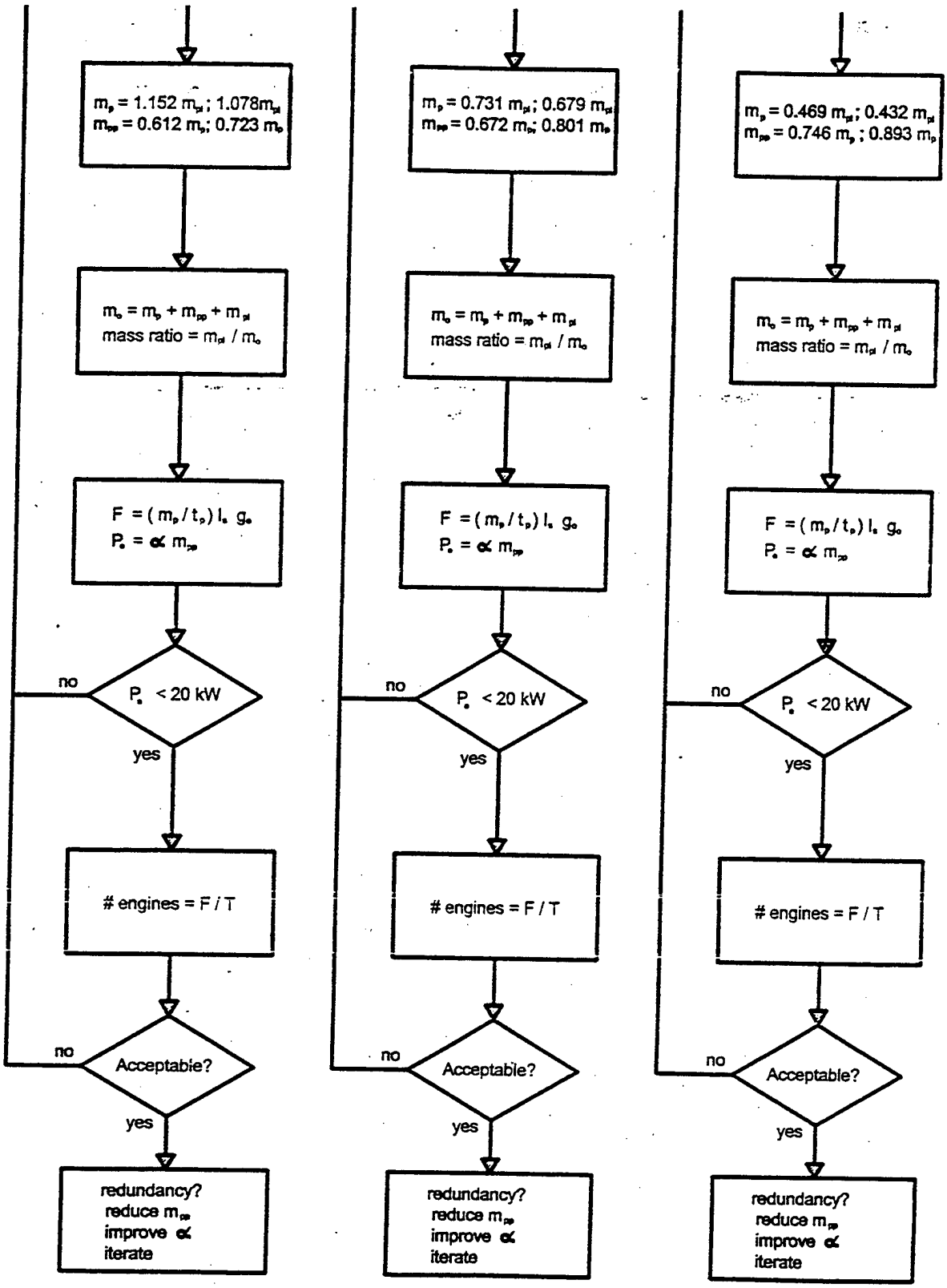
$m_p = 1.152\ m_{pl}$; $1.078 m_{pl}$
$m_{pp} = 0.612\ m_p$; $0.723\ m_p$
$m_o = m_p + m_{pp} + m_{pl}$
mass ratio = m_{pl} / m_o
$F = (m_p / t_p)\ I_s\ g_o$
$P_e = \alpha\ m_{pp}$
no
P_e < 20 kW
yes
engines = F / T
no
Acceptable?
yes
redundancy?
reduce m_{pp}
improve α
iterate
$m_p = 0.731\ m_{pl}$; $0.679\ m_{pl}$
$m_{pp} = 0.672\ m_p$; $0.801\ m_p$
$m_o = m_p + m_{pp} + m_{pl}$
mass ratio = m_{pl} / m_o
$F = (m_p / t_p)\ I_s\ g_o$
$P_e = \alpha\ m_{pp}$
no
P_e < 20 kW
yes
engines = F / T
no
Acceptable?
yes
redundancy?
reduce m_{pp}
improve α
iterate
$m_p = 0.469\ m_{pl}$; $0.432\ m_{pl}$
$m_{pp} = 0.746\ m_p$; $0.893\ m_p$
$m_o = m_p + m_{pp} + m_{pl}$
mass ratio = m_{pl} / m_o
$F = (m_p / t_p)\ I_s\ g_o$
$P_e = \alpha\ m_{pp}$
no
P_e < 20 kW
yes
engines = F / T
no
Acceptable?
yes
redundancy?
reduce m_{pp}
improve α
iterate

V. APPLICATION OF METHOD

Note: In the following three examples, the defined parameters which had to be estimated by the author are preceded by the symbol "~".

A. "LIGHT" LEO TO GEO MISSION

For a particular LEO to GEO satellite, the following parameters are defined:

mission velocity requirement, $\Delta u = 4200$ m/s

payload mass, $m_{pl} = 250$ kg

mission time, t_m = unrestricted / reasonable.

Using the defined optimization procedure, three potentially optimized engine runs are attempted at payload mass ratios of $m_{pl} / m_o = 0.35$, 0.45, and 0.55.

In this example, the second ("tankage" considered) case for the payload mass ratio of 0.45, proves to be the optimized profile. Note that approximately 10 to 12 engines are required if the H_2 arcjet is selected as the thruster for this profile.

This example demonstrates that fuel tank mass considerations lead to the addition of more thrusters in order to compensate for the added mass. The mass penalty is easily scalable.

IDEAL:

$m_{pl} / m_o = 0.35$

$I_s = 829$ sec
engine selected:
NH_3 Arcjet
$I_s = 650$ sec
$\alpha = 320$ W/kg
$\eta_t = 0.32$
T = 0.2 N

$t_p = 5.28 \times 10^5$ sec
$= 6.11$ days
$t_p < t_m$

$m_p = 270$ kg
$m_{pp} = 195.2$ kg
$m_o = 715$ kg
payload ratio checks

F = 3.26 N; $P_e = 63$ kW
$\therefore$ 17 engines required;
power req. excessive

with TANKAGE...
$I_s = 972$ sec
engine selected:
H_2 Arcjet
$I_s = 1000$ sec
$\alpha = 333$
$\eta_t = 0.4$
T = 0.2 – 0.25 N

$t_p = 4.71 \times 10^5$ sec
$= 5.45$ days
$t_p < t_m$

$m_p = 270$ kg
$m_{pp} = 195.2$ kg
$m_o = 715$ kg
payload ratio checks

F = 5.47 N; $P_e = 65$ kW
$\therefore$ 22 to 28 engines
required

$m_{pl} / m_o = 0.45$

$I_s = 1075$ sec
engine selected:
NASA / Primex EO-1
$I_s = 1150$ sec
$\alpha = 20$ W/kg
$\eta_t = 0.098$
T = pulsed

$t_p = 4.21 \times 10^7$ sec
$= 487$ days
$t_p < t_m$

$m_p = 182.8$ kg
$m_{pp} = 122.8$ kg
$m_o = 556$ kg
payload ratio checks

F = 0.0490 N; $P_e = 3$ kW
$\therefore$ 1,919 engines
required!!!

$I_s = 1250$ sec
engine selected:
H_2 Arcjet
$I_s = 1000$ sec
$\alpha = 333$
$\eta_t = 0.4$
T = 0.2 – 0.25 N

$t_p = 7.07 \times 10^5$ sec
$= 8.18$ days
$t_p < t_m$

$m_p = 169.8$ kg
$m_{pp} = 136.0$ kg
$m_o = 556$ kg
payload ratio checks

F = 2.36 N; $P_e = 46$ kW
$\therefore$ 10 to 12 engines
required; power high

$m_{pl} / m_o = 0.55$

$I_s = 1439$ sec
engine selected:
ARC SPT-100
$I_s = 1600$ sec
$\alpha = \sim 169.8$W/kg
$\eta_t = 0.48$
T = 0.083 N

$t_p = 1.638 \times 10^6$ sec
$= 19.0$ days
$t_p < t_m$

$m_p = 117.3$ kg
$m_{pp} = 87.5$ kg
$m_o = 455$ kg
payload ratio checks

F = 1.011 N; $P_e = 15$ kW
$\therefore$ 13 engines required

$I_s = 1687$ sec
engine selected:
Hall (Xe)
$I_s = 15$-1600 sec
$\alpha = 150$
$\eta_t = 0.5$
T = 0.04 N

$t_p = 2.04 \times 10^6$ sec
$= 23.6$ days
$t_p < t_m$

$m_p = 108.0$ kg
$m_{pp} = 96.4$ kg
$m_o = 454$ kg
payload ratio checks

F = 0.831N; $P_e = 15$ kW

$\therefore$ 21 engines required

B. "HEAVY" LEO TO GEO (COMM SAT) MISSION

Given a LEO to GEO mission for the orbit raising of a communication satellite, the optimization algorithm requires that we initially define the payload and required Δu for the transit.

The payload is defined to be relatively massive, weighing 1000 kg, and the defined Δu for the transfer is approximately 4640 m/s. For this mission, the transfer time cannot be unrealistically excessive due to the general mission urgency of communication satellite tasking. Using the planning algorithm, the results are illustrated as shown on the following page.

This example provides some interesting results. First, the payload is extremely heavy for most electrical propulsion engines. As stated in the earlier chapters, most high thrust electric propulsion engines are still in development. Yet, the Hall TAL D-55 engine is capable of accomplishing this mission in 88½ days with only 11 engines – excluding redundancy.

In both of the cases at the payload mass ratio of 0.45, it is evident that the increased burn time to maintain the profile allows for fewer engines as less thrust is required over a longer time. None-the-less, the number of engines required for this profile as $m_{pl} / m_o = 0.45$ is unacceptable.

IDEAL:

$m_{pl} / m_o = 0.35$

$I_s = 916$ sec
engine selected:
NASA/Primex EO-1
$I_s = 1150$ sec
$\alpha = \sim 20$ W/kg
$\eta_t = 0.098$
T = pulsed

$t_p = 3.37 \times 10^7$ sec
$= 389$ days
$= 1.067$ years

SHOWSTOPPER...
due $t_p >> t_m$

$m_{pl} / m_o = 0.45$

$I_s = 1187$ sec
engine selected:
Hall (Xe)
$I_s = 15$ -1600 sec
$\alpha = 150$ W/kg
$\eta_t = 0.5$
T = 0.04 N

$t_p = 1.342 \times 10^6$ sec
$= 15.54$ days
$t_p < t_m$

$m_p = 731$ kg
$m_{pp} = 491$ kg
$m_o = 2222$ kg
payload ratio checks

F = 8.02 N; $P_e = 74$ kW
$\therefore$ 201 engines required!

$m_{pl} / m_o = 0.55$

$I_s = 1589$ sec
engine selected:
Hall TAL D-55
$I_s = 1600$ sec
$\alpha = \sim 50.9$ W/kg
$\eta_t = 0.48$
T = 0.082 N

$t_p = 6.67 \times 10^6$ sec
$= 77.1$ days
$t_p < t_m$

$m_p = 469$ kg
$m_{pp} = 350$ kg
$m_o = 1819$ kg
payload ratio checks

F = 1.104 N; $P_e = 18$ kW
$\therefore$ 14 engines required

with TANKAGE...

$I_s = 1074$ sec
engine selected:
H_2 Arcjet
$I_s = 1000$ sec
$\alpha = 333$ W/kg
$\eta_t = 0.4$
T = 0.2 – 0.25 N

$t_p = 5.75 \times 10^5$ sec
$= 6.65$ days
$t_p < t_m$

$m_p = 1078$ kg
$m_{pp} = 779$ kg
$m_o = 2857$ kg
payload ratio checks

F= 18.39 N; P_e= 259 kW
$\therefore$ 74 to 92 engines
required!!!

$I_s = 1381$ sec
engine selected:
Hall (Xe)
$I_s = 15$ -1600 sec
$\alpha = 150$ W/kg
$\eta_t = 0.5$
T = 0.04 N

$t_p = 1.533 \times 10^6$ sec
$= 17.74$ days
$t_p < t_m$

$m_p = 679$ kg
$m_{pp} = 544$ kg
$m_o = 2223$ kg
payload ratio checks

F = 6.52 N; $P_e = 82$ kW
$\therefore$ 163 engines required!

$I_s = 1864$ sec
engine selected:
Hall TAL D-55
$I_s = 1600$ sec
$\alpha = \sim 50.9$ W/kg
$\eta_t = 0.48$
T = 0.082 N

$t_p = 7.65 \times 10^6$ sec
$= 88.5$ days
$t_p < t_m$

$m_p = 432$ kg
$m_{pp} = 386$ kg
$m_o = 1818$ kg
payload ratio checks

F = 0.886 N; P_e= 20 kW
$\therefore$ 11 engines required

C. LEO TO MARS MISSION

For a representative LEO to Mars mission, the optimization algorithm requires that we initially define the payload and required Δu.

The payload is defined to be a relatively small probe (mass equal to 250 kg), and the defined Δu for the transfer is approximately 5,700 m/s. In this case, Δu also defines a mission time (t_m) equal to 256 days. Thus, in order for the calculations to be valid, the burn time (t_b) must not exceed t_m.

The results of the calculations are demonstrated as shown.

Note that for the third case of $m_{pl} / m_o = 0.55$ either of the steady MPD thrusters would have been a better specific impulse fit. Those engines are scaleable in the range from $I_s = 2000$ to 5000 sec. However, since they are presently still under development, they have been excluded from this analysis even though it is strongly anticipated that such engines will be the desired propulsion systems for deep-space missions.

IDEAL:

$m_{pl} / m_o = 0.35$

$I_s = 1125$ sec
engine selected:
Teflon PPT (pulsed)
$I_s = 1000$ sec
$\alpha = 1.0$ W/.kg
$\eta_t = 0.07$
T = pulsed

$t_p = 1.422 \times 10^9$ sec
= 16,457 days
= 45 years!!!

SHOWSTOPPER...
due $t_p >> t_m$

$m_{pl} / m_o = 0.45$

$I_s = 1458$ sec
engine selected:
Hall SPT (Xe)
$I_s = 1500$ sec
$\alpha = 150$ W/kg
$\eta_t = 0.5$
T = 0.04 N

$t_p = 2.03 \times 10^6$ sec
= 23.4 days
$t_p < t_m$

$m_p = 182.7$ kg
$m_{pp} = 122.8$ kg
$m_o = 556$ kg
payload ratio checks

F = 1.324 N; $P_e = 19$ kW
$\therefore$ 34 engines required

$m_{pl} / m_o = 0.55$

$I_s = 1952$ sec
engine selected:
SPT-100 (Fakel)
$I_s = 1600$ sec
$\alpha = 150$ W/kg
$\eta_t = 0.48$
T = 0.083 N

$t_p = 3.42 \times 10^6$ sec
= 39.5 days
$t_p < t_m$

$m_p = 117.3$ kg
$m_{pp} = 87.5$ kg
$m_o = 455$ kg
payload ratio checks

F = 0.538 N; $P_e = 14$ kW
$\therefore$ 7 engines required

with TANKAGE...

$I_s = 1319$ sec
engine selected:
Hall (Xe)
$I_s = 15\text{-}1600$ sec
$\alpha = 150$ W/kg
$\eta_t = 0.5$
T = 0.04 N

$t_p = 1.540 \times 10^6$ sec
= 17.83 days
$t_p < t_m$

$m_p = 270$ kg
$m_{pp} = 195.2$ kg
$m_o = 715$ kg
payload ratio checks

F = 2.58 N; $P_e = 30$ kW
$\therefore$ 65 engines required;
power required is high

$I_s = 1697$ sec
engine selected:
ARC SPT-100
$I_s = 1600$ sec
$\alpha = 131.4$ W/kg
$\eta_t = 0.48$
T = 0.083 N

$t_p = 2.75 \times 10^6$ sec
= 31.8 days
$t_p < t_m$

$m_p = 169.8$ kg
$m_{pp} = 136.0$ kg
$m_o = 556$ kg
payload ratio checks

F = 0.969 N; $P_e = 18$ kW
$\therefore$ 12 engines required

$I_s = 2289$ sec
engine selected:
XIPS
$I_s = 28\text{-}3500$ sec
$\alpha = 100$ W/kg
$\eta_t = 0.75$
T = 0.015-0.04 N

$t_p = 3.76 \times 10^6$ sec
= 43.5 days
$t_p < t_m$

$m_p = 108.0$ kg
$m_{pp} = 96.4$ kg
$m_o = 454$ kg
payload ratio checks

F = 0.789 N; $P_e = 10$ kW
$\therefore$ 20 to 53 engines
required

VI. CONCLUSIONS AND RECOMMENDATIONS

A. CONCLUSIONS

Routine implementation of electric propulsion for space thrusting applications is relatively new even though the governing concepts are almost 40 years old. The very latest engines, presented as examples in this thesis, demonstrate that some aspects of electric propulsion are still in their early stages of development. However, in light of time-tested theory and the limitations of chemical propulsion systems, it is evident that, right now, electric propulsion is the only potential stepping-stone to deep-space probes or other craft that could conceivably travel the great distances between the planets and beyond the solar system.

For any such mission profiles – interplanetary or interstellar in particular – the propulsion systems for these missions will have to be optimized. Such engines will have to be cost-effective, thrust efficient and therefore mass minimized. Someday there may even be considerations to make these systems potentially re-useable and refuelable. This thesis presents one technique with which mission profiles and engine selection can be matched and consequently optimized to theoretically achieve the greatest benefit of least overall mass with both maximum fuel and maximum payload in order to achieve the shortest mission time for a given payload.

Thus, a primary focus of this thesis has been to provide a new way of looking at electrical propulsion systems design in addition to attempting to provide an up-to-date and comprehensive summary of available electric propulsion thruster data. The selected approach (i.e., the Langmuir-Irving formulation) is based upon first principles as well as an analysis of other methods that are currently in use. In essence, an objective has been

to produce a design alternative to the satellite design engineers. This methodology or "procedure" is intended to generate some consideration into performance near a pre-determined yet not inflexible "dual-optimum" point. It is apparent in the literature that aspects of the discussed "dual-optimum" point have been plotted in various texts and somewhat addressed but never fully explored.

The most important concept to note is the idea that these results are "theoretical" in that systems are currently designed according to algorithms that are based more solidly on operational experience and power considerations than on any approach that considers pure optimization. In essence, no design algorithm is really in use that seems to consider optimization. Granted, electric propulsion is still in its early stages and most applications involving satellite re-positioning and orbit-lifting do not place heavy lift nor aggressive profile constraints upon engines. Consequently, such considerations or additional restraints may not really be required.

Due to the relatively limited number of electrical propulsion engines that are currently operational, the examples of this thesis show that it is sometimes difficult to find an identical match to an optimum profile's specific impulse, I_s. In fact, some of the most powerful and most promising electric propulsion engines – those most likely to be desirable for high thrust and high payload mass missions – are still in some stages of development.

Specific impulse, I_s, is comparable to the required "gas mileage" for a particular trip through space. After the profile is determined through orbital mechanics, the required incremental change in vehicular velocity (Δu) is known. Then, the required tank of fuel can be established for an expected level of performance or fuel efficiency – "gas

mileage." Hence, the objective is to match the profile to specific impulse (or engine). This is accomplished using the "dual-optimum" procedure. Nonetheless, the "dual-optimum" establishes not only I_s but also suggests desired values of specific power (α) and thruster efficiency (η_t) as well as the likely burn time (t_p) for a desired mission profile, Δu.

As demonstrated in the three provided examples in the previous chapter, it is not obvious how a particular engine will perform on a specific mission profile. In essence, the design optimum is dependent as much on the payload mass (m_{pl}) and mass payload ratio (m_{pl} / m_o) as upon the specific characteristic of the engine itself.

The most important of these engine characteristics are specific power (α), thruster efficiency (η_t), and available thrust (T). Specific power, α, is the most critical to the designer because it drives the amount of available power to the thruster versus the required mass of the overall system that provides that power. As power conditioning systems improve and the "state-of-the-art" in the field advances, this parameter will improve and enhance electrical propulsion system performance. In this thesis, it is evident that specific power has been the most difficult parameter to establish for the majority of the listed engines. A worked example demonstrates that this is primarily due to the fact that the value given to α varies depending somewhat upon arbitrary considerations such as thruster configuration, redundancy, etc. In addition, it shows that mass reduction is equally as important as where that mass is "billed" within the calculations.

Thruster efficiency, η_t, generates a feel for the engine's efficiency in terms of nozzle losses, off-axis losses, as well as other thruster inefficiencies. Generally, these

values vary widely depending upon the type of thruster under consideration. For example, the LES 8/9 PPT thruster has an efficiency of only 0.0068 to 0.009 while the N_2H_4 resistojet turns in numbers in the 0.8 to 0.9 range. The reasons for this are discussed in depth.

Available thrust, T, although extremely small on most electrical propulsion systems, gives a measure of the number of engines required for a necessary profile. This value can be a major player as demonstrated in the examples because it drives largely the additional issues of component redundancy and additional mass – which again affects alpha, α.

Another consideration which became apparent in the course of this work is the capability to allow for the required fuel tanks within the design and thus within the optimum profile. Fuel considerations are certainly mission or profile dependent. Consequently, this is a substantial capability for the designer to predict optimum performance with variable tank mass as per mission requirements.

These results, as presented, are easily scalable depending upon the particular profile and its fuel requirements. Exploration of the topic of allowing for "tankage" created estimation possibilities that allowed for even more realistic comparisons between different electric propulsion systems. As evident in the overall engine parameter summary in Table 5, some engines (of the pulsed MPD variety) require no fuel storage tanks at all.

If the engine summary shows one thing, it certainly lets one know that there are a host of possibilities out there being developed by aggressive companies. These systems use a variety of physical principles to create thrust. Some at greater expense of the other

relevant parameters -- α, η_t, and T. Consequently, the examples provided for the design algorithm (on the three different mission profiles) demonstrate that all engines are not created equal for various mission profiles – certainly not if one endeavors to fly an optimum profile.

Of course, industry may argue that there are important additional considerations on any profile. For example, a communication satellite that takes six months to be in position is probably not cost-effective. That could be a mission failure. Nonetheless, success depends on what parameter is being optimized. In the case of this research, the objective was to optimize both the mass and time constraints. At the present time, in the development of the "state-of-the-art" in the evolution of electrical propulsion, this was not always possible. This fact is certainly demonstrated in the examples provided, which show that there are no obvious trends with the systems currently available. Electric propulsion is not totally there yet; however, scientists and engineers are pushing the frontier forward and expanding to new horizons and possibilities.

B. RECOMMENDATIONS

In any branch of research involving a rapidly growing technology (particularly one in which corporate vendors on the "cutting-edge" of that technology are especially unwilling to give up data that they consider proprietary), it is extremely difficult to track the leading edge of developments. Consequently, acquiring the latest available data can be next to impossible. Hence, best-estimate scenarios can be flawed or only approximate.

In the course of this research, the author frequently ran into barriers when attempting to answer questions regarding particular thruster systems. A more open forum could certainly benefit not only science but also the vendors themselves, particularly if

the data contained within this thesis proves useful to designers. On the other hand, the developed procedure might demonstrate that certain engines are less effective for necessary mission profiles. As a result, one design might prove less effective than another.

Additional work could be extremely advantageous if a more in-depth study could be made into attempting to combine the various schools of thought in design criteria. Like missile design, there is no clear-cut or established method that is followed due to the fact that a design must consider the whole picture – i.e., mass, time, and power considerations – all at once. Considerations of power, time, and cost seem to be the biggest factors in design at the present time, and obviously contractors wanting to sell their products are not going to be quick to admit that a system could be better optimized with another company's thruster. Certainly, perfection is infinitely expensive, but that is not what this process advocates. Systems could simply be better if any attempt were made to "ride the dual-optimum profile." The author would certainly be curious if industry were to consider the presented ideas and improve upon them.

APPENDIX A. DEVELOPMENT - PAYLOAD MASS FRACTION EQUATION:

By definition, specific power, $\alpha = P_e / m_{pp}$. Thus, $m_{pp} = P_e / \alpha$. (Sutton, 1992, pg. 597)

By definition, electrical power available (as previously shown), $P_e = m_p v^2 / (2 t_p \eta_t)$. Hence, $m_{pp} = (1/\alpha) (m_p v^2 / (2 t_p \eta_t))$. Solving for payload mass, m_p, yields... $m_p = m_{pp} (2 \alpha t_p \eta_t / v^2)$ or $m_{pp} / m_p = v^2 / 2 \alpha t_p \eta_t$. (Sutton, 1992, pg. 596)

By definition of allocated spacecraft masses, $m_o = m_p + m_{pl} + m_{pp}$. Define final mass, $m_f = m_o - m_p$ (i.e. initial mass less propellant mass). Thus, redefine initial mass as follows: $m_o = m_p + m_f$. (Sutton, 1992, pg. 596)

Derived from the equation for maximum velocity at propellant burnout, $\Delta u = v \ln (m_o / m_f)$, know that $e^{\Delta u/v} = m_o / m_f = m_o / (m_o - m_p) = 1 / (1 - m_p / m_o)$. This equation, when solved for m_p / m_o, gives $m_p / m_o = 1 - e^{-\Delta u/v}$. (Sutton, 1992, pg. 123)

Rewriting the equation for initial mass yields $m_o = m_p (1 + m_{pp} / m_p) + m_{pl}$. Now, when substituting the above equation for m_{pp} / m_p, the initial mass is rewritten as follows: $m_o = m_p (1 + v^2 / 2 \alpha t_p \eta_t) + m_{pl}$.

Again, rewriting the equation... $1 = (m_p / m_o) (1 + v^2 / 2 \alpha t_p \eta_t) + m_{pl} / m_o$. Substituting the equation for m_p / m_o and solving for m_{pl} / m_o, the equation transforms to $m_{pl} / m_o = 1 - (1 - e^{-\Delta u/v}) (1 + v^2 / 2 \alpha t_p \eta_t)$.

When this equation is multiplied through and solved for m_{pl}/m_o , the payload mass fraction appears as illustrated: $m_{pl} / m_o = (1 - (v / v_c)^2 (e^{\Delta u/v} - 1)) / e^{\Delta u/v}$.

THIS PAGE INTENTIONALLY LEFT BLANK.

APPENDIX B. FIRST PRINCIPLES – CODES

The following three pages contain the MATLAB codes that were utilized in the generation of Figures 2, 3, and 4 respectively.

```
%  THESIS
%  Plot2(2):  mpl / mo  vs.  v / vc
%         "payload fraction vs. v / vc"

%  LT John Jay De Bellis, USN
%  30 JUN 99

%  variables:
%          x() = v / vc
%          a() = deltau / vc
%          y() = mpl / mo


x1=linspace(0,3,300)
x2=linspace(0,3,300)
x3=linspace(0,3,300)
a1=0.2
a2=0.3
a3=0.5
y1=(1-x1.^2 .* (exp(a1./x1)-1))./exp(a1./x1)
y2=(1-x2.^2 .* (exp(a2./x2)-1))./exp(a2./x2)
y3=(1-x3.^2 .* (exp(a3./x3)-1))./exp(a3./x3)

figure(1), plot(x1,y1,x2,y2,x3,y3), grid
axis([0 3 0.0 1.0])
ylabel('mpl / mo'),xlabel('v / vc')
gtext('deltau/vc = 0.2'), gtext('deltau/vc = 0.3'), gtext('deltau/vc = 0.5')
```

```
%  THESIS
%  Plot1:  deltau / vc vs. v / vc (or Is / vc)
%         "incremental change of vehicle velocity vs. impulse"

%  LT John Jay De Bellis, USN
%  25 AUG 99

%  Variables:
%          x() = v / vc
%          a() = mpl / mo
%          y() = deltau / vc

x1=linspace(0,3,300)
x2=linspace(0,3,300)
x3=linspace(0,3,300)

a1=0.35
a2=0.45
a3=0.55

y1=x1.*log((1 + x1.^2)./(a1 + x1.^2))
y2=x2.*log((1 + x2.^2)./(a2 + x2.^2))
y3=x3.*log((1 + x3.^2)./(a3 + x3.^2))

figure(1), plot(x1,y1,x2,y2,x3,y3), grid
axis([0.0 2.0 0.0 0.5])
ylabel('deltau / vc'),xlabel('v / vc')
gtext('mpl/mo = 0.35'), gtext('mpl/mo = 0.45'), gtext('mpl/mo = 0.55')
```

```
%  THESIS
%  Plot3:  optimization curves -- joint optimum
%         "product of incremental change of vehicle velocity and payload ratio vs.
%                                  specific impulse" (mpl/mo * deltau vs. Is)

%  LT John Jay De Bellis, USN
%  25 AUG 99

%  Variables:
%          x() = v / vc
%          a() = mpl / mo
%          y() = deltau / vc

x1=linspace(0,3,300)
x2=linspace(0,3,300)
x3=linspace(0,3,300)

a1=0.35
a2=0.45
a3=0.55

y1=x1.*log((1 + x1.^2)./(a1 + x1.^2))
y2=x2.*log((1 + x2.^2)./(a2 + x2.^2))
y3=x3.*log((1 + x3.^2)./(a3 + x3.^2))

%z1=y1.*a1
%z2=y2.*a2
%z3=y3.*a3

figure(1), plot(x1,y1,x2,y2,x3,y3), grid
axis([0.1 0.15 0.5 1.5])
ylabel('deltau/vc * mpl/mo'), xlabel('v/vc')
gtext('mpl/mo = 0.35'), gtext('mpl/mo = 0.45'), gtext('mpl/mo = 0.55')
```

APPENDIX C. DUAL OPTIMUM CODE

This appendix lists the necessary Maple program code that is utilized in the production of Figure 4, which illustrates the "dual optimum."

THESIS: Plot #5: OPT. CURVES: 3-D plot: optimization of v/vc and mpl/mo curves

LT John Jay De Bellis, USN
30 JUN 1999

defined variables:
deltau = defined incremental change of vehicle velocity (m/s) -- defined by mission
vc = characteristic velocity (m/s)
v = effective exhaust velocity (m/s)
mratio = payload ratio = mpl/mo

x = v/vc
y = mpl/mo

```
> restart; with(plots); with(plottools);
  plot3d(x*y*ln((1+x^2)/(y+x^2)),x=0.5..1.3,y=0.3..0.6,axes=BOXED,ti
  tle="optimization:  product of v/vc and mpl/mo");
```

[*animate, animate3d, animatecurve, changecoords, complexplot, complexplot3d, conformal, contourplot, contourplot3d, coordplot, coordplot3d, cylinderplot, densityplot, display, display3d, fieldplot, fieldplot3d, gradplot, gradplot3d, implicitplot, implicitplot3d, inequal, listcontplot, listcontplot3d, listdensityplot, listplot, listplot3d, loglogplot, logplot, matrixplot, odeplot, pareto, pointplot, pointplot3d, polarplot, polygonplot, polygonplot3d, polyhedra_supported, polyhedraplot, replot, rootlocus, semilogplot, setoptions, setoptions3d, spacecurve, sparsematrixplot, sphereplot, surfdata, textplot, textplot3d, tubeplot*]

[*arc, arrow, circle, cone, cuboid, curve, cutin, cutout, cylinder, disk, dodecahedron, ellipse, ellipticArc, hemisphere, hexahedron, homothety, hyperbola, icosahedron, line, octahedron, pieslice, point, polygon, project, rectangle, reflect, rotate, scale, semitorus, sphere, stellate, tetrahedron, torus, transform, translate, vrml*]

APPENDIX D. TANKAGE PENALTY CODES

The following pages list the MAPLE program codes that were used in the creation of Figures 6 and 7 respectively.

```
%  THESIS
%  Plot1T:  deltau / vc vs. v / vc (or Is / vc) with 10% TANKAGE PENALTY
%         "incremental change of vehicle velocity vs. impulse"

%  LT John Jay De Bellis, USN
%  25 AUG 99

%  Variables:
%          x() = v / vc
%          a() = mpl / mo
%          y() = deltau / vc

x1=linspace(0,3,300)
x2=linspace(0,3,300)
x3=linspace(0,3,300)

a1=0.35
a2=0.45
a3=0.55

y1=x1.*log((1.1 + x1.^2)./(a1 + x1.^2 + 0.1))
y2=x2.*log((1.1 + x2.^2)./(a2 + x2.^2 + 0.1))
y3=x3.*log((1.1 + x3.^2)./(a3 + x3.^2 + 0.1))

figure(1), plot(x1,y1,x2,y2,x3,y3), grid
axis([0.0 2.0 0.0 0.5])
ylabel('deltau / vc'),xlabel('v / vc')
gtext('mpl/mo = 0.35'), gtext('mpl/mo = 0.45'), gtext('mpl/mo = 0.55')
```

```
%  THESIS
%  Plot1T:  deltau / vc vs. v / vc (or Is / vc) with/without 10% TANKAGE PENALTY
%         "incremental change of vehicle velocity vs. impulse"

%  LT John Jay De Bellis, USN
%  25 AUG 99

%  Variables:
%          x() = v / vc
%          a() = mpl / mo
%          y() = deltau / vc

x1=linspace(0,3,300)
x2=linspace(0,3,300)
x3=linspace(0,3,300)

a=0.45

y1=x1.*log((1.1 + x1.^2)./(a + x1.^2 + 0.1))
y2=x2.*log((1 + x2.^2)./(a + x2.^2))

figure(1), plot(x1,y1,x2,y2), grid
axis([0.0 2.0 0.0 0.5])
ylabel('deltau / vc'),xlabel('v / vc')
gtext('mpl/mo = 0.45'), gtext('mpl/mo = 0.45 with 10% tankage penalty')
```

THIS PAGE INTENTIONALLY LEFT BLANK.

LIST OF REFERENCES

Agrawal, B. N., *Design of Geosynchronous Spacecraft*, Prentice-Hall, Inc., 1986.

Auweter-Kurtz, Kurtz, Schrader, "Optimization of Electric Propulsion Systems Considering Specific Power as Function of Specific Impulse," *Journal of Propulsion and Power*, Vol. 4, No. 6, pp. 512-519, November-December 1988.

Clauss, C., Atlantic Research Corporation, 19 July 1999.
Electronic correspondence between Mr. Craig Clauss (clauss@arceng.com), Atlantic Research Corporation, and the author, 19 July 1999.

Filliben, J. D., "Electric Propulsion for Spacecraft," *CPIA Bulletin*, Vol. 22, No. 5, pp. 4-5, September 1996.

Filliben, J. D., "Electric Thruster Systems Enter 'Era of Application'," *CPIA Bulletin*, Vol. 23, No. 5, pp. 5-8, September 1997.

Hill, P. G. and Peterson, C. R., *Mechanics and Theory of Propulsion*, 2d ed., Addison-Wesley Publishing Company, Inc., 1992.

Humble, R. W., Henry, G. N., and Larson, W. J., *Space Propulsion Analysis and Design*, The McGraw-Hill Companies, Inc., 1995.

Langmuir, D. B., "Low-thrust Flight: Constant Exhaust Velocity in Field-free Space," *Space Technology (edited byH. S. Siefert)*, Chapman and Hall Limited, 1959.

Martinez-Sanchez, M. and Pollard, J. E., "Spacecraft Electric Propulsion – An Overview," *Journal of Propulsion and Power*, Vol. 14, No. 5, pp. 688-699, September-October 1998.

"Navy's Hall Thruster Electric Propulsion System Goes Operational," Naval Space Command Space Tracks, pg. 13, March-April 1999.

Oleson, S., "On-board Propulsion Branch Home Page."
[http://www.lerc.nasa.gov/WWW/onboard/onboard.html]. May 1999.

Osborn, Mike, Naval Research Labs, 14 June 1999.
Electronic correspondence between Mr. Mike Osborn (mosborn@space.nrl.navy.mil), Naval Research Labs and the author, 14 June 1999.

Sackheim, R. L. and Byers, D. C., "Status and Issues Related to In-space Propulsion Systems," *Journal of Propulsion and Power*, Vol. 14, No. 5, pp. 669-675, September-October 1998.

Santarius, J. F., "Plasma and Electric Propulsion."
[http://elvis.neep.visc.edu/~jfs/neep602.lect31.97/plasmaprop.html]. November 1997.

Sutton, G. P., *Rocket Propulsion Elements*, John Wiley & Sons, Inc. 1992.

BIBLIOGRAPHY

Archer, R. D. and Saarlar, M., *An Introduction to Aerospace Propulsion*, Prentice-Hall, Inc., 1996.

Garrison, P. W. and Stocky, J. F., "Future Spacecraft Propulsion," AIAA-88-0406, Nov-Dec 1988.

Zucker, R. D., *Fundamentals of Gas Dynamics*, Matrix Publishers, Inc., 1977.

THIS PAGE INTENTIONALLY LEFT BLANK.